AWARD NUMBER: W81XWH-14-1-0480

TITLE: Androgen receptor splice variants and resistance to taxane chemotherapy

PRINCIPAL INVESTIGATOR: Haitao Zhang

CONTRACTING ORGANIZATION: Tulane University, New Orleans, LA 70112

REPORT DATE: October 2015

TYPE OF REPORT: Annual

PREPARED FOR: U.S. Army Medical Research and Materiel Command
Fort Detrick, Maryland 21702-5012

REPORT DOCUMENTATION PAGE

Form Approved
OMB No. 0704-0188

1. REPORT DATE	2. REPORT TYPE	3. DATES COVERED
October 2015	Annual	29/09/2014-28/09/2015

4. TITLE AND SUBTITLE

Androgen receptor splice variants and resistance to taxane chemotherapy

5a. CONTRACT NUMBER
W81XWH-14-1-0480

5b. GRANT NUMBER

5c. PROGRAM ELEMENT NUMBER

6. AUTHOR(S)
Haitao Zhang, Ph.D.

E-Mail:hzhang@tulane.edu

5d. PROJECT NUMBER

5e. TASK NUMBER

5f. WORK UNIT NUMBER

7. PERFORMING ORGANIZATION NAME(S) AND ADDRESS(ES)

Tulane University
1430 Tulane Ave
New Orleans, LA 70112

8. PERFORMING ORGANIZATION REPORT NUMBER

9. SPONSORING / MONITORING AGENCY NAME(S) AND ADDRESS(ES)

U.S. Army Medical Research and Materiel Command
Fort Detrick, Maryland 21702-5012

10. SPONSOR/MONITOR'S ACRONYM(S)

11. SPONSOR/MONITOR'S REPORT NUMBER(S)

12. DISTRIBUTION / AVAILABILITY STATEMENT

Approved for Public Release; Distribution Unlimited

13. SUPPLEMENTARY NOTES

14. ABSTRACT

During the first reporting period, we have made significant progress in understanding the fundamental difference in nuclear translocation mechanism between full-length androgen receptor (AR-FL) and AR splice variants (AR-Vs). We found that the AR-FL is associated with the microtubule cytoskeleton and is transported by the microtubules prior to its nuclear translocation. On the other hand, AR-V7 and AR^{v567es} have weak microtubule-binding activities and use a microtubule-independent mechanism for intracellular transport. Through a series of deletion analyses, we have mapped the microtubule-binding activity to two regions in the AR ligand-binding domain. In addition, we found that AR-V7 and AR^{v567es} interfere with docetaxel-mediated AR-FL cytoplasmic retention, possibly by forming heterodimers with AR-FL and decreasing its microtubule-binding activity. These findings provide evidence that constitutively active AR-Vs maintain the AR signaling axis by evading the inhibitory effects of microtubule-targeting agents, suggesting that these AR-Vs play a role in resistance to taxane chemotherapy.

15. SUBJECT TERMS
Castration-resistant prostate cancer; docetaxel; cabazitaxel; chemotherapy; androgen receptor splice variants; microtubule; ligand-binding domain; nuclear translocation

16. SECURITY CLASSIFICATION OF:			17. LIMITATION OF ABSTRACT	18. NUMBER OF PAGES	19a. NAME OF RESPONSIBLE PERSON
a. REPORT	b. ABSTRACT	c. THIS PAGE			USAMRMC
Unclassified	Unclassified	Unclassified	Unclassified	35	19b. TELEPHONE NUMBER *(include area code)*

Table of Contents

Page

1. Introduction

Docetaxel-based chemotherapy is established as a first-line treatment and standard of care for patients with metastatic castration-resistant prostate cancer (mCRPC). However, half of the patients do not respond to treatment and those do respond eventually become refractory. A better understanding of the resistance mechanisms to taxane chemotherapy is both urgent and clinical significant, as taxanes (docetaxel and cabazitaxel) are being used in various clinical settings. Sustained signaling through the androgen receptor (AR) has been established as a hallmark of CRPC. Recently, several alternative splicing variants of AR (AR-Vs) that lack the ligand-binding domain (LBD) have been identified. Preliminary studies conducted in our laboratory showed increased expression of AR-Vs (AR-V7 and AR^{v567es}) rendered prostate cancer cells less responsive to taxane drugs. The objective of this application is to test the hypothesis that constitutively active AR-Vs are associated with resistance to taxane chemotherapy in CRPC.

2. Keywords

Castration-resistant prostate cancer; docetaxel; cabazitaxel; chemotherapy; androgen receptor splice variants; microtubule; ligand-binding domain; nuclear translocation; importin

3. Accomplishments

What are the major goals/tasks of this project?

Major Task 1: To determine if ectopic expression of caARVs in tumor xenografts reduces the sensitivity to taxanes.
Major Task 2: To determine if knockdown of caARV sensitizes LNCaP95 and LuCaP 136 xenografts to taxanes.
Major Task 3: To identify the microtubule-associated sequence (MTAS) on AR.
Milestone: Identify the sequence of AR that is involved in microtubule-binding. Publish 1 peer-reviewed paper.
Major Task 4: To conduct a clinical study to evaluate the correlation between caARVs expression and response to taxane chemotherapy in patients treated for mCRPC.

What was accomplished under these goals?

Major Task 3: To identify the microtubule-associated sequence (MTAS) on AR

Our preliminary studies demonstrated that the nuclear import of full-length AR (AR-FL) depends on a dynamic microtubule, whereas that of the AR-Vs is microtubule-independent (1). We hypothesize that this fundamental difference is caused by the different binding capacities to the microtubule cytoskeleton by the two types of receptors. This hypothesis was confirmed by using an in vivo microtubule-binding assay (1). In addition, we generated a series of deletion constructs encompassing different domains of AR. By using the in vivo microtubule-binding assay, we have demonstrated that the

microtubule-binding is mediated by the ligand-binding domain (1). Consistent with this finding, we found that the LBD-truncated AR-V7 and AR^{v567es} both bind poorly to the microtubules (1).

To further map the region(s) within the LBD that is responsible for microtubule association, we created a series of deletion constructs within the LBD (Fig. 1A). COS-7 cells transfected with these plasmids were cultured in an androgen-deprived condition and lysed for the in vivo microtubule-binding assay, and the results are summarized in Table 1. The deletion analysis suggest that there are two regions in the LBD that are potentially involved in binding to the microtubules, located within a.a. 732-774 and a.a. 815-889, respectively (Fig. 1A). Interestingly, fragments containing one or two copies of the putative MTAS showed similar MT-binding activities (Table 1 and Fig. 1), suggesting functional redundancy.

Table 1. Summary of AR-LBD deletion analysis.

Name	LBD fragment	MT binding*	Localization (w/o androgen)
AR-FL	666-919	++	Cytoplasmic
ΔC1	666-858	++	Cytoplasmic
ΔC2	666-795	++	Cytoplasmic
ΔC3	666-774	++	Cytoplasmic
ΔC4	666-754	-	Nuclear
ΔC5	666-732	-	Nuclear
ΔN1	732-919	++	Cytoplasmic
ΔN2	795-919	++	Cytoplasmic
ΔN3	815-919	++	Cytoplasmic
ΔN4	858-919	-	Nuclear
ΔNC1	732-795	++	Cytoplasmic
ΔNC2	785-889	++	Cytoplasmic

*, scored based on relative MT-binding activity compared to that of AR-FL. ++, >75%; +, 50-75%; -, <50%.

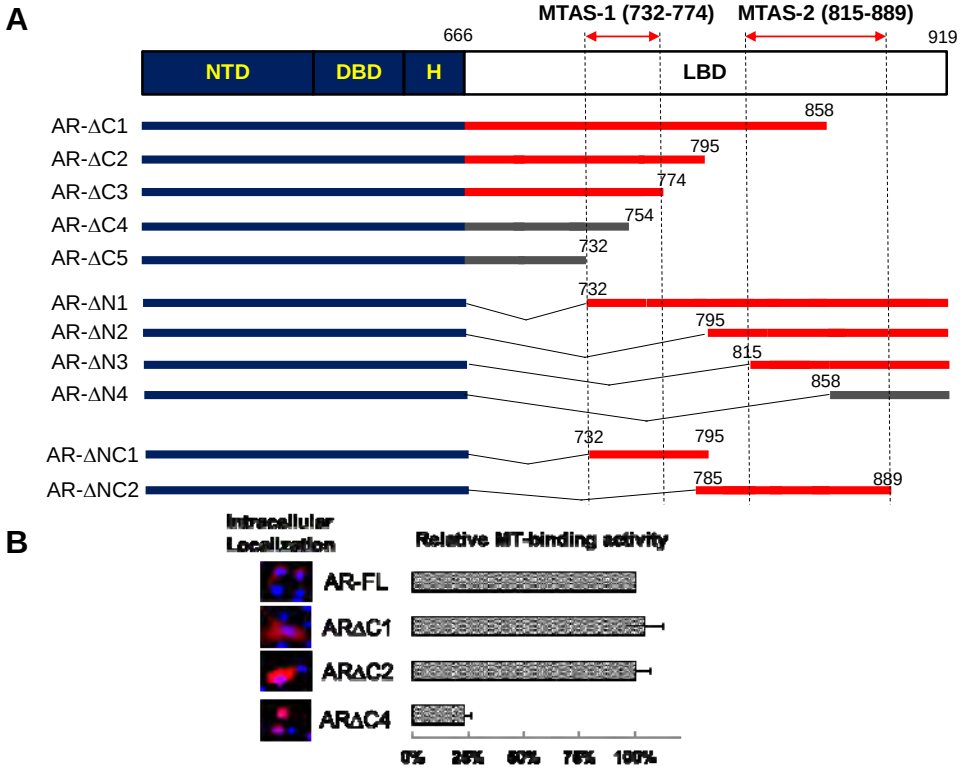

Figure 1. A, diagram of the deletion constructs containing various fragments of the ligand-binding domain. Fragments with strong microtubule-binding activities are shown in red. Two putative microtubule association sequences (MTAS) are shown. **B,** microtubule-binding activity (right) and intracellular localization (left) of selected AR-LBD mutants. AR was stained with an anti-N-terminus antibody and a secondary antibody conjugated with Alexa Fluor 594 (red). Nuclei were stained with DAPI (blue). The full summary is provided in Table 1.

Additionally, the intracellular localization of these proteins were analyzed by immunofluorescence using an antibody recognizing the N-terminus of AR. As shown by Fig 1B and Table 1, when the cells were cultured in the absence of androgens, the mutants that are capable of microtubule-binding were located in the cytoplasm, whereas those with weak binding activities were localized to the nucleus. Similar observations were made with AR-V7 and AR^{v567es}, which possess weak microtubule-binding activities but translocate to the nucleus in a constitutive manner (1). These results suggest the functional significance of the microtubules in controlling the intracellular localization of AR. Lacking the MTAS may allow the splice variants to escape cytoplasmic retention by the microtubules.

Additional work related to Task 3. In addition to the work proposed under Task 3, we made the following discoveries which are related to Task 3:

1. AR-V7 and AR^{v567es} interfere with docetaxel-mediated AR-FL cytoplasmic retention (1), possibly by forming heterodimers with AR-FL (2) and decreasing its microtubule-binding activity (1).
2. The nuclear import of AR-V7 and AR^{v567es} was blocked by an importin β inhibitor, importazole, suggesting both variants are imported to the nucleus by the importin α/β machinery (1).

Summary for Task 3: we have identified two regions in the AR LBD that are involved in microtubule-binding. We have also published one research article in Oncotarget. Thus, we have achieved the milestone listed under Major Task 3.

Task 4: To conduct a clinical study to evaluate the correlation between AR-Vs expression and response to taxane chemotherapy in patients treated for mCRPC.

Evaluation of protocols for detecting AR-Vs in the blood. We evaluated the whole-blood approach (whole-blood collected in Paxgene Blood RNA tubes, also referred to as the PAXgene approach) and the CTC negative selection approach based on depletion of CD45+ leukocytes (also referred to as the CD45-depletion approach). Ten heavily treated mCRPC patients were identified for this purpose and blood samples obtained from the same patient were analyzed by both approaches (Fig. 2). As shown in Table 2, AR-FL and AR-V7 transcripts were detected in all samples by both methods. AR^{v567es} was detected in 20% of the samples by the PAXgene approach, but only in 10% by the CD45-depletion, suggesting that the leukocyte depletion process may cause a loss of sensitivity. Indeed, the AR-Vs transcript levels measured by

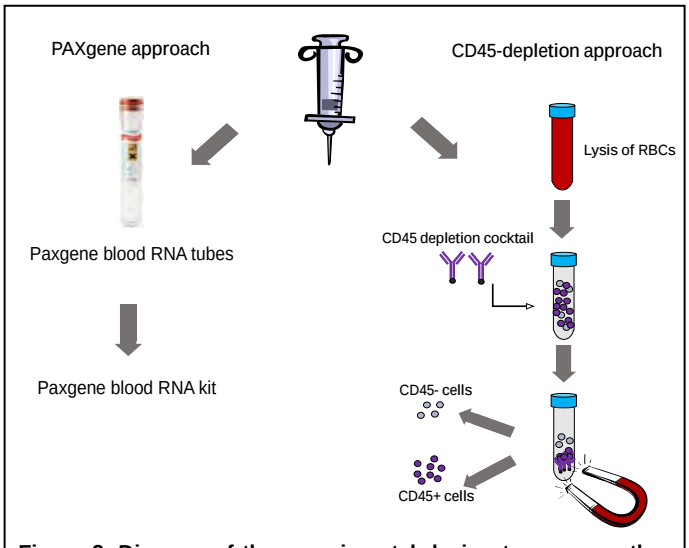

Figure 2. Diagram of the experimental design to compare the PAXgene approach with the CD45-depleteion approach.

the CD45-depletion approach were always lower than those by the PAXgene approach: in the case of AR-V7, the estimated loss of sensitivity was ~40% (Table 3).

Table 2. Detection of AR transcripts by two approaches.

	PAXgene	CD45 depletion
AR-FL	10/10	10/10
AR-V7	10/10	10/10
AR^{v567es}	2/10	1/10

The separation of CD45- and CD45+ cells during the leukocyte depletion process provides an opportunity to investigate the sources of AR transcripts in the blood. As shown in Table 4, in the majority of the samples (8 out of 10), the AR-V7 transcript was exclusively from the CD45- fraction. Only 2 out of 10 samples were with detectable AR-V7 in the CD45+ fraction. The expression level, when compared to the CD45- fraction (i.e. CTC-enriched fraction), were markedly lower. Similarly, the vast majority of AR^{v567es} transcript was found in the CD45- fraction. In contrast, AR-FL is abundantly expressed in the both fractions (Table 4).

Table 3. Relative expression levels of AR-V transcripts by CD45-depletion approach as compared to the PAXgene approach.

Sample ID	Relative expression (%)*	
	AR-V7	AR^{v567es}
1	33.06	-
2	18.04	-
3	78.75	-
4	54.55	92.34
5	73.50	-
6	60.42	0
7	85.71	-
8	29.32	-
9	80.15	-
10	84.73	-
Mean±SD	59.82 ± 21.10	**-**

***The expression level detected by the PAXgene approach is set as 100%.

Collectively, these results suggest that the AR-Vs transcripts in the CD45+ fraction are below or slightly above the level of detection, suggesting that depleting the hematopoietic cells offers little or no improvement in specificity for the detection of AR-Vs. On the other hand, performing this procedure could lead to a loss of sensitivity, possibly due to RNA degradation during the process.

Table 4. Distribution of AR transcripts in the CD45- and CD45+ fractions*.

ID	AR-V7		AR^{v567es}		AR-FL	
	CD45-	CD45+	CD45-	CD45+	CD45-	CD45+
1	100.00%	0.00%	-	-	46.05%	53.95%
2	100.00%	0.00%	-	-	29.21%	70.79%
3	100.00%	0.00%	-	-	63.96%	36.04%
4	85.93%	14.07%	96.16%	3.84%	55.55%	44.45%
5	100.00%	0.00%	-	-	65.27%	34.73%
6	100.00%	0.00%	-	-	54.75%	45.25%
7	100.00%	0.00%	-	-	20.02%	79.98%
8	91.65%	8.35%	-	-	76.71%	23.29%
9	100.00%	0.00%	-	-	75.59%	24.41%
10	100.00%	0.00%	-	-	31.34%	68.66%

***The percentage values were calculated from the expression ratio between the two fractions, with a total of 100%.

Sensitivity of the PAXgene assay. Based on the results above, we decided on the PAXgene approach for AR-V detection in blood. To estimate the sensitivity of this assay, fixed numbers of 22Rv1 cells, which express a number of AR-Vs including AR-V7, were

spiked into 5 ml blood from a healthy donor. Fig. 3 shows that this assay has the sensitivity of detecting 5-50 AR-V7+ cells in 5 ml of blood, or 1-10 cells per ml of blood.

Summary for Major Task 4: we have developed the sample collection procedure for detecting the expression of AR-Vs in blood. In addition, we have also developed the digital PCR protocol for AR-Vs detection. Patient selection and sample collection are ongoing.

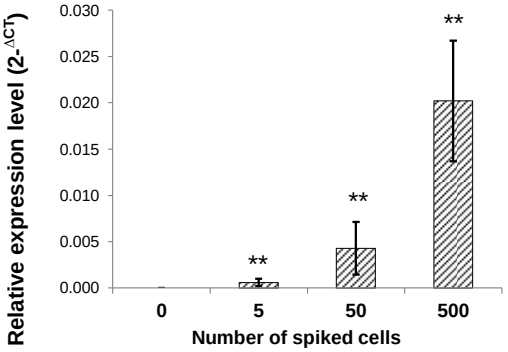

Figure 3. Sensitivity of the PAXgene approach in detection of AR-V7 mRNA. Specified numbers of 22RV1 cells were spiked into 5 ml of blood from a healthy donor and transferred to PAXgene tubes. RNA was purified using the PAXgene Bloood RNA Kit and qRT-PCR was performed. Statistics analysis was performed using one-tailed Z-test. **, P<0.01.

What opportunities for training and professional development has the project provided?

Nothing to report.

How were the results disseminated to communities of interest?

Nothing to report.

What do you plan to do during the next reporting period to accomplish the goals?

Due to the departure of Xichun Liu, the proposed animal studies under Major Tasks 1 and 2 were delayed. In the next reporting period, we will start the animal studies and continue the clinical study under Major Task 4.

Citations (published journal articles):

1. Zhang G, Liu X, Li J, Ledet E, Alvarez X, Qi Y, et al. Androgen receptor splice variants circumvent AR blockade by microtubule-targeting agents. Oncotarget. 2015;6:23358–71.

2. Xu D, Zhan Y, Qi Y, Cao B, Bai S, Xu W, et al. Androgen Receptor Splice Variants Dimerize to Transactivate Target Genes. Cancer Res. 2015;75:3663–71.

4. Impact

What was the impact on the development of the principal discipline(s) of the project?

Despite the availability of new treatment options in recent years, treating mCRPC remains a critical challenging. The survival benefits of these new treatments (abirtaterone, enzalutamide, etc) are moderate and patients will become refractory. Taxanes are currently being prescribed in various clinical settings, including treating mCRPC patients who have progressed after these new treatments. Therefore, improving and prolong the efficacy of taxanes is a viable and practical approach in the clinical management of CRPC. The results from this project thus far suggest AR-Vs are associated with resistance to taxane chemotherapy. The clinical impact is that the status of AR-Vs expression could be used as

a biomarker to match patient with treatment, therefore have a significant impact on the mortality and morbidity of CRPC. The identification and characterization of the microtubule-binding sequence in the AR-LBD could deepen our understanding of the regulatory network controlling the intracellular localization and trafficking of AR.

What was the impact on other disciplines?

Nothing to report.

What was the impact on technology transfer?

Nothing to report.

What was the impact on society beyond science and technology?

Nothing to report.

5. Changes/Problems

Dr. Xichun Liu, who is an expert on animal studies, accepted a position in the in the industry during the first reporting period. Dr. Liu's depart has caused delay in the planned animal studies. We are in the process of identifying a candidate with animal expertise.

6. Products

Publications, conference papers, and presentations

- **Journal publications.** The following two papers were published:

  Zhang G, Liu X, Li J, Ledet E, Alvarez X, Qi Y, et al. Androgen receptor splice variants circumvent AR blockade by microtubule-targeting agents. Oncotarget. 2015;6:23358–71. Status: Published; Acknowledgement of federal support: yes.

  Xu D, Zhan Y, Qi Y, Cao B, Bai S, Xu W, et al. Androgen Receptor Splice Variants Dimerize to Transactivate Target Genes. Cancer Res. 2015;75:3663–71. Status: Published; Acknowledgement of federal support: yes.

- **Books or other non-periodical, one-time publications.** Nothing to report.

- **Other publications, conference papers, and presentations.** Presentations:

  Haitao Zhang. Constitutively active androgen receptor splice variants circumvent AR blockade by microtubule-targeting agents in prostate cancer. Invited talk. The First Affiliated Hospital of the Medical College of Xi'an Jiaotong University, Xi'an, China. June 11, 2015.

  Haitao Zhang. Androgen receptor splice variants circumvent AR blockade by microtubule-targeting agents in prostate cancer. Invited talk. Jilin University School of Basic Medicine, Changchun, Jilin. June 9, 2015.

Xichun Liu, Elisa Ledet, Yanfeng Qi, Yan Don, Oliver Sartor, and **Haitao Zhang**: A Novel Blood-Based Assay for Detecting Androgen Receptor Splice Variants in Patients with Advanced Prostate Cancer. Poster presentation. American Urological Association Annual Meeting 2015, May 15, 2015

Xichun Liu, Guanyi Zhang, Jianzhuo Li, Elisa Ledet, Yanfeng Qi, Yan Don, Oliver Sartor, and **Haitao Zhang**: Constitutively Active Androgen Receptor Splice Variants Confer Resistance to Taxane Chemotherapy in Prostate Cancer. Poster presentation. Society of Basic Urological Research Annual Symposium, November 15, 2014.

Haitao Zhang. Androgen receptor splice variants and chemoresistance in castration-resistant prostate cancer. Invited talk. UT Southwest Medical Center, Dallax, TX. November 12, 2014.

Xichun Liu, Elisa Ledet, Yanfeng Qi, Yan Don, Oliver Sartor, and **Haitao Zhang**. A Novel Blood-Based Assay for Detecting Androgen Receptor Splice Variants in Patients with Advanced Prostate Cancer. Poster presentation. Prostate Cancer Foundation Scientific Retreat, October 23, 2014

Website(s) or other Internet site(s)

Nothing to report.

Technologies or techniques

Nothing to report.

Inventions, patent applications, and/or licenses

Nothing to report.

Others

Nothing to report.

7. Participants & Other Collaborating Organizations

What individuals have worked on the project?

Name	Haitao Zhang	Guanyi Zhang	Xichun Liu	Elisa Ledet	Brian Lewis
Project role	PI	Technician	Postdoctoral Fellow	Study coordinator	Co-investigator
Researcher Identifier (ORCID ID)	0000-0002-5969-1024	N.A.	N.A.	N.A.	N.A.
Nearest person month worked	3	9	3	0.5	0.5
Contribution to project	Project design; data analysis; Study coordination; presentation; manuscript writing; report	Identification of MTAS;	Developing sample collection and ddPCR protocols	Clinical study coordinator	Patient recruitment and consent
Funding support	DOD-PCRP, Louisiana Board of Regents, American Cancer Society	Louisiana Board of Regents, American Cancer Society	DOD-PCRP, American Cancer Society	DOD-Postdoctoral Fellowship	

Has there been a change in the active other support of the PD/PI(s) or senior/key personnel since the last reporting period?

Nothing to report.

What other organizations were involved as partners?

Nothing to report.

8. Special Reporting Requirements: not applicable.

9. Appendices

1). Zhang G, Liu X, Li J, Ledet E, Alvarez X, Qi Y, et al. Androgen receptor splice variants circumvent AR blockade by microtubule-targeting agents. Oncotarget. 2015;6:23358–71.

2). Xu D, Zhan Y, Qi Y, Cao B, Bai S, Xu W, et al. Androgen Receptor Splice Variants Dimerize to Transactivate Target Genes. Cancer Res. 2015;75:3663–71.

Androgen receptor splice variants circumvent AR blockade by microtubule-targeting agents

Guanyi Zhang[1,2,6], Xichun Liu[2,6], Jianzhuo Li[1,2,6], Elisa Ledet[4,5,6], Xavier Alvarez[7], Yanfeng Qi[3,6], Xueqi Fu[1], Oliver Sartor[4,5,6], Yan Dong[1,3,6], Haitao Zhang[2,6]

[1]College of Life Sciences, Jilin University, Changchun, P.R. China

[2]Department of Pathology, Tulane University School of Medicine, New Orleans, Louisiana, USA

[3]Department of Structural and Cellular Biology, Tulane University School of Medicine, New Orleans, Louisiana, USA

[4]Department of Medicine, Tulane University School of Medicine, New Orleans, Louisiana, USA

[5]Department of Urology, Tulane University School of Medicine, New Orleans, Louisiana, USA

[6]Tulane Cancer Center, Tulane University School of Medicine, New Orleans, Louisiana, USA

[7]Division of Comparative Pathology, Tulane National Primate Research Center, Covington, Louisiana, USA

Correspondence to:
Haitao Zhang, **e-mail:** hzhang@tulane.edu

Keywords: androgen receptor, splice variants, prostate cancer, taxane chemotherapy, microtubule

Received: *April 24, 2015* ***Accepted:*** *June 09, 2015* ***Published:*** *June 22, 2015*

ABSTRACT

Docetaxel-based chemotherapy is established as a first-line treatment and standard of care for patients with metastatic castration-resistant prostate cancer. However, half of the patients do not respond to treatment and those do respond eventually become refractory. A better understanding of the resistance mechanisms to taxane chemotherapy is both urgent and clinical significant, as taxanes (docetaxel and cabazitaxel) are being used in various clinical settings. Sustained signaling through the androgen receptor (AR) has been established as a hallmark of CRPC. Recently, splicing variants of AR (AR-Vs) that lack the ligand-binding domain (LBD) have been identified. These variants are constitutively active and drive prostate cancer growth in a castration-resistant manner. In taxane-resistant cell lines, we found the expression of a major variant, AR-V7, was upregulated. Furthermore, ectopic expression of two clinically relevant AR-Vs (AR-V7 and AR^{V567es}), but not the full-length AR (AR-FL), reduced the sensitivities to taxanes in LNCaP cells. Treatment with taxanes inhibited the transcriptional activity of AR-FL, but not those of AR-Vs. This could be explained, at least in part, due to the inability of taxanes to block the nuclear translocation of AR-Vs. Through a series of deletion constructs, the microtubule-binding activity was mapped to the LBD of AR. Finally, taxane-induced cytoplasm sequestration of AR-FL was alleviated when AR-Vs were present. These findings provide evidence that constitutively active AR-Vs maintain the AR signaling axis by evading the inhibitory effects of microtubule-targeting agents, suggesting that these AR-Vs play a role in resistance to taxane chemotherapy.

INTRODUCTION

Prostate cancer is the most common non-skin cancer and the second leading cause of cancer mortality in men in the United States. Androgen deprivation therapy, which disrupts androgen receptor (AR) signaling by reducing androgen levels through surgical or chemical castration, or by administration of anti-androgens that compete with androgens for binding to AR [1], is the first-line treatment for metastatic and locally advanced prostate cancer. While this regimen is effective initially, progression to the presently incurable and lethal stage, termed castration-resistant prostate cancer (CRPC), invariably occurs. In 2004, docetaxel-based chemotherapy is established as a first-line treatment and standard of care for patients with metastatic CRPC [2]. However, about half of the patients

do not respond to treatment and those do respond become refractory within one year. Several new treatments, including the new taxane cabazitaxel [3], the CYP17A1 inhibitor abiraterone [4], and the potent antiandrogen enzalutamide [5], have received FDA approval as second-line treatments for metastatic CRPC in recent years. However, the survival benefits are relatively small (< = 5 months) and patients eventually become refractory to treatments. Therefore, breakthroughs in the treatment of prostate cancer hinge upon better understandings of the mechanisms of therapeutic resistance of CRPC.

Paclitaxel, docetaxel, and cabazitaxel belong to the taxane family of chemotherapeutic agents. Taxanes bind to the microtubules and prevent their disassembly, thereby suppressing microtubule dynamics, leading to mitotic arrest and apoptosis [6]. This was believed to be the mechanism of action of taxanes in prostate cancer until recently when it was demonstrated by several groups that taxanes in fact inhibit the AR signaling pathway in prostate cancer. Taxanes have been shown to block the nuclear translocation of AR and inhibit the expression of AR-regulated genes [7, 8]. Additionally, Gan et al. showed that taxanes inhibit the transcriptional activity of AR by inducing FOXO1, a transcriptional repressor of AR [9]. It is well-established that CRPC cells remain addicted to AR signaling; therefore, the inhibitory effect on AR, rather than the antimitotic activity, could possibly be the predominant mechanism of action for taxanes in prostate cancer.

Sustained signaling through AR has been established as a hallmark of CRPC. Recently, alternative splicing variants of AR (AR-Vs) that lack the ligand-binding domain (LBD) have been identified [10–13]. These splice variants remain transcriptionally active in the absence of androgens and drive prostate cancer growth in a castration-resistant manner. In addition, these variants are reported to be prevalently upregulated in CRPC compared to hormone-naïve prostate cancer [10–13]. AR-Vs can regulate the expression of canonical androgen-responsive genes, as well as a unique set of target genes [12, 14]. In a significant portion of metastatic CRPC tissues, the variants proteins are expressed at a level comparable to that of the canonical, full-length AR (AR-FL) [15, 16]. Patients with high expression of two major AR-Vs, AR-V7 (also known as AR3) and AR^{v567es}, have shorter cancer-specific survival than other CRPC patients [15]. In addition, recent studies have provided strong support for a critical role of these AR-Vs in resistance to hormonal therapies, including enzalutamide and abiraterone [17–20].

Recently, laboratory and clinical studies have suggested the existence of a cross-resistance mechanism between taxane-based chemotherapy and second-line hormonal therapies [21–25]. In this study, we set out to test the potential roles of AR-Vs in modulating the response to taxane-based chemotherapy.

RESULTS

Taxane-resistant prostate cancer cell lines express higher levels of AR-V7

We first established taxane-resistant 22Rv1 and LNCaP95 lines by culturing cells in escalating doses of paclitaxel and docetaxel over a period of 2 months. The response to taxanes were determined by the MTT assay (Fig. 1, A–C). Western blotting analyses showed that the expression of AR-FL was reduced, whereas the expression of AR-V7 was robustly induced, in the 22Rv1 resistant lines in comparison with the passage-matched parental line (Fig. 1D). A similar, albeit less pronounced, induction of AR-V7 was observed in the LNCaP95 docetaxel-resistant line (Fig. 1E). These results suggest that the constitutive active AR-V7 was selectively up-regulated in taxane-resistant prostate cancer cells.

Expression of constitutively active AR-Vs impairs the cytotoxicity of taxanes

To directly test the roles of constitutively active AR-Vs in resistance to taxanes, we transfected AR-V7 and AR^{v567es} into the AR-V-null LNCaP cells, and measured the responses to taxanes. As shown in Fig. 2A, cell viability after docetaxel treatment was markedly higher in cells expressing AR-V7 or AR^{v567es}, but not in those overexpressing AR-FL, than in vector-transfected cells. Similar observations were made with paclitaxel and cabazitaxel (Supplementary Figure S1). In LNCaP95 cells, when the expression of AR-V7 was silenced by a V7-specific shRNA, cells became more sensitive to docetaxal and cabazitaxel (Fig. 2B). Taken together, these results suggest the expression of constitutively active AR-Vs negatively impacts the efficacies of taxanes in prostate cancer cells.

Transcriptional activities of the constitutively active AR-Vs are refractory to the taxanes

To understand the difference between AR-V7/AR^{v567es} and the AR-FL in cytoprotection against the taxanes, we investigated the influence of taxane treatment on the transactivation activities of these AR isoforms. COS-7, which does not express any AR proteins, was chosen in this experiment to avoid interference from the endogenous AR. As shown in Fig. 3, treatment with docetaxel or paclitaxel dose-dependently inhibited the ligand-dependent transcriptional activity of AR-FL, but neither drug was able to inhibit the constitutive activities of AR-V7 and AR^{v567es}. This disparity can't be attributed to the down-regulation of AR-FL expression, as all AR proteins were not affected by the treatments (Supplementary Figure S2). These results suggest that the transcriptional activities of the AR variants are refractory to the inhibitory effects of taxanes.

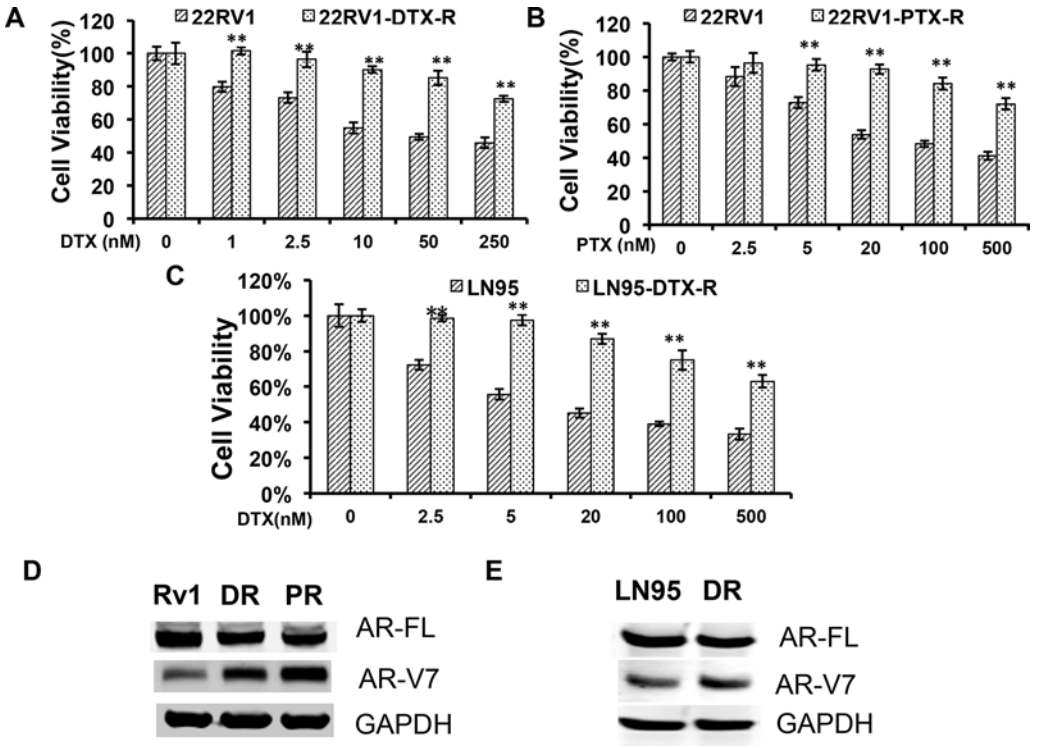

Figure 1: Upregulation of AR-V7 in taxane-resistant prostate cancer cells. A. and **B.** 22Rv1 with acquired resistance to taxanes were established by culturing in escalating doses of docetaxel (DTX) or paclitaxel (PTX). MTT assays were performed in passage-matched 22Rv1 or 22Rv1 resistant cells to determine the responses to taxanes. **C.** The response of DTX-resistant LNCaP95 to docetaxel treatment. **D.** and **E.** Western blotting using an anti-N terminal antibody or an AR-V7-specific antibody in 22Rv1 (D) or LNCaP95 (E) resistant cells. Rv1/LN95, passage-matched parental line; DR, docetaxel-resistant; PR, paclitaxel-resistant. The *P* values were determined by the *Student's t*-tests, ** denotes $P < 0.01$. The results presented are mean ± SEM from three experiments.

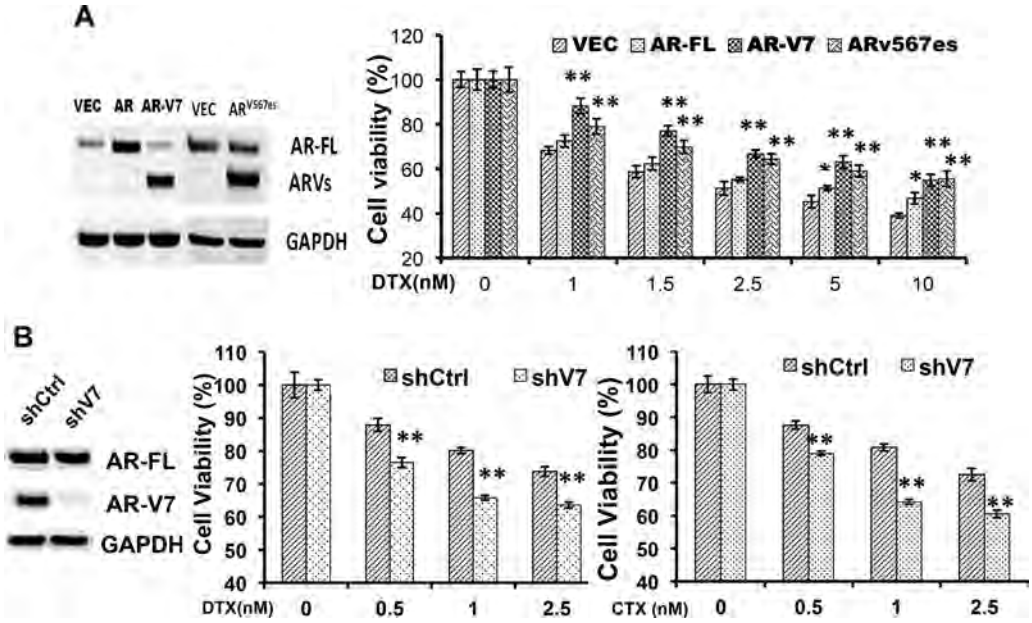

Figure 2: Expression of constitutively active AR-Vs negatively impact the cytotoxicities of taxanes. A. LNCaP cells were transfected with vector, AR-FL, AR-V7, or AR^{v567es}, and cell viability was determined by the MTT assay after 48 h of treatment with docetaxel. Western analysis was performed with an antibody recognizes the N-terminus of AR. The *P* values were determined by the *Student's t*-tests. *$P < 0.05$; **$P < 0.01$ vs vector. **B.** LNCaP95 cells were cultured in an androgen-depleted condition, and transfected with a control or an AR-V7-specific shRNA. **$P < 0.01$. CTX, cabazitaxel. The results presented are mean ± SEM.

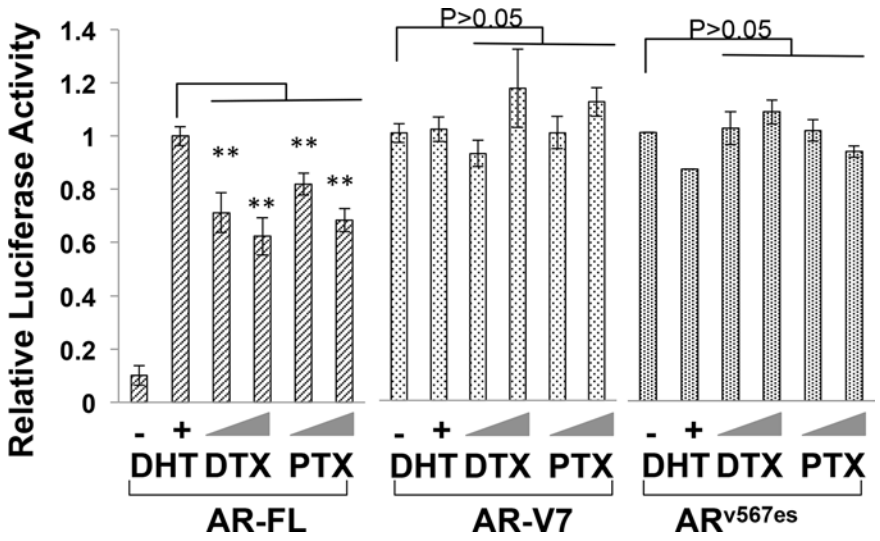

Figure 3: Transcriptional activities of constitutively active AR-Vs are refractory to taxane treatment. COS-7 cells were transfected with the ARR3-luc reporter plasmid along with a plasmid encoding AR-FL, AR-V7, or AR^{v567es}. The luciferase reporter assay was performed after 24 h treatment. The *P* values were determined by the *Student's t*-tests. $^{**}P < 0.01$ vs untreated. Doses: DTX, 1 and 2.5 nM; PTX, 2.5 and 5 nM. The results presented are mean ± SEM from three experiments.

Nuclear imports of constitutively active AR-Vs are microtubule-independent

Next, we investigated the influence of the taxanes on nuclear translocation of AR-V7 and AR^{v567es}, as these agents have been shown to block that of AR-FL [7, 8]. Enhanced green fluorescent protein (EGFP)-tagged AR-FL and AR-V7 were expressed in COS-7 cells and the localization of the fusion proteins was analyzed by fluorescence microscopy. Unlike EGFP-AR-FL, which required androgen stimulation for nuclear import, EGFP-AR-V7 spontaneously translocated to the nucleus (Supplementary Figure S3). When docetaxel and paclitaxel were added to the culture medium following androgen stimulation, accumulation of AR-FL in the cytoplasm was observed after 24 h of treatment (Supplementary Figure S3). However, treatment with the taxanes had no effect on the subcellular distribution of AR-V7.

To validate the results above, we performed fluorescence recovery after photobleaching (FRAP) assays in COS-7 cells expressing fluorescence-tagged AR proteins. Following treatment with docetaxel, selected nuclei were photobleached and the cells were imaged at regular intervals. Nuclear translocation is indicated by recovery of the nuclear to cytoplasmic fluorescence ratio (Fn/c). As indicated by the confocal images (Fig. 4A) and the fractional recovery plots (Fig. 4B), nuclear import of AR-FL was greatly deterred by docetaxel. In contrast, the nuclear translocations of AR-V7 and AR^{v567es} were not affected by docetaxel, evidenced by similar Fn/c recovery curves in control and treated cells (Fig. 4B). To substantiate these findings, we performed FRAP assays with additional microtubule inhibitors. KX-01 is a novel peptidomimetic inhibitor of Src family of kinases, but also inhibits tubulin polymerization [26], and nocodazole causes microtubule disassembly [27]. Once again, these drugs inhibited the nuclear import of AR-FL, but not that of AR-V7 or AR^{v567es} (Fig. 4B). Collectively, these results suggest the nuclear translocation of AR-V7 or AR^{v567es} are not mediated by the microtubules.

AR associates with the microtubules through the LBD

Proteins that use the microtubule pathway for nuclear import are known to bind to the microtubules [28, 29]. To test whether AR binds to the microtubules, we conducted *in vivo* microtubule-binding assays in COS-7 cells ectopically expressing AR. Under the condition in which the microtubules were stabilized, the majority of AR-FL co-precipitated with the microtubules and was found in the pellet (Fig. 5). Importin β was used as a negative control as previously described [29], and p53, which is known to be a microtubule-binding protein [30], was used as the positive control. The microtubule-binding activity was quantitated by the pellet to supernatant (P/S) ratio [29]. In contrast, when nocodazole, $CaCl_2$, or low temperature was employed to disrupt microtubule integrity, AR-FL shifted from the pellet to the supernatant, leading to marked decreases of the P/S ratios. These results suggest the AR-FL is a microtubule-associated protein.

To map the region responsible for microtubule-binding on AR, we generated a series of deletion constructs encompassing different domains of AR (Fig. 6, left panel). These constructs were analyzed by the microtubule binding assay. As shown in

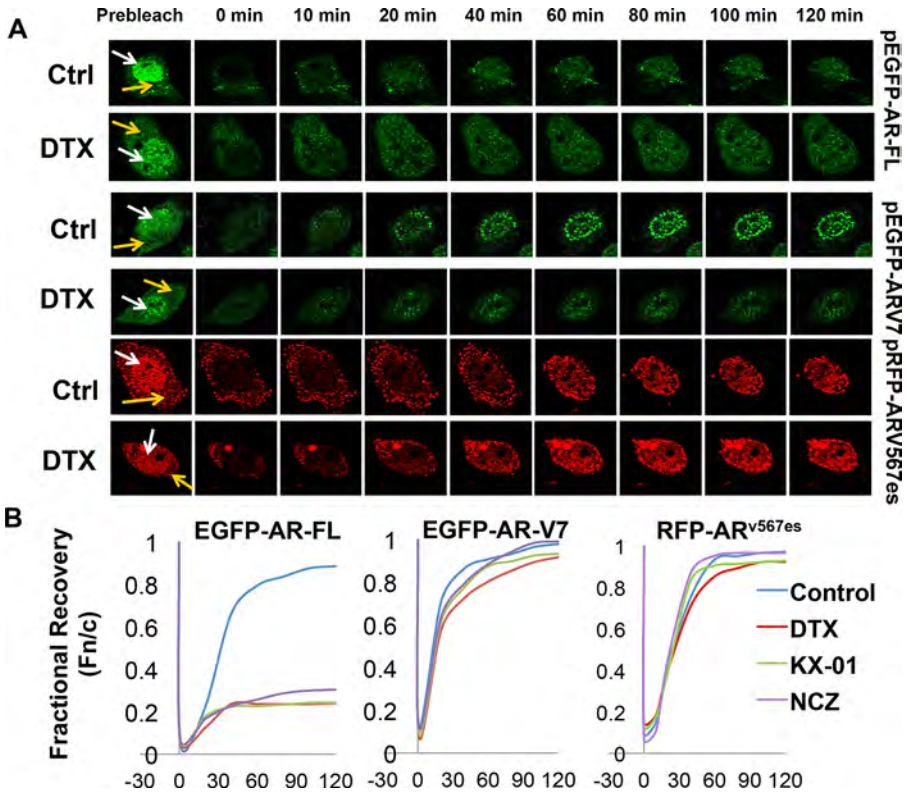

Figure 4: Nuclear imports of constitutively active AR-Vs are microtubule-independent. FRAP assays were performed in COS-7 cells expressing different fluorescence-tagged AR proteins. Cells transfected with EGFP-AR-FL were cultured in the presence of androgen. Cells were treated with 20 nM docetaxel for 2 h before photobleaching. **A.** Confocal images taken at different intervals after photobleaching of the nuclei. White and yellow arrows indicate the nucleus and the cytoplasm, respectively. **B.** Recovery plot of the nuclear:cytoplamic fluorescence ratio (Fn/c) over time in cells treated with different microtubule inhibitors. Fn/c ratios are expressed as fractions of the pre-photobleach Fn/c. Nocodazole (NCZ) was used at 5 μg/ml and KX-01 was at 100 nM. FRAP images for NCZ and KX-01 are in Supplementary Figure S4.

Supplementary Figure S4A and Figure 6 (right panel), all constructs lacking the LBD have poor microtubule-binding activities. In contrast, those retaining the LBD have similar binding activities as that of AR-FL (Supplementary Figure S4B and Figure 6). These results indicate that microtubule association is mediated by the LBD. Consistent with this finding, we found that the LBD-truncated AR-V7 and AR^{v567es} both bind poorly to the microtubules (Fig. 7).

AR-Vs interfere with docetaxel-mediated AR-FL cytoplasmic retention

It has been previously shown that both AR-V7 and AR^{v567es} facilitate AR-FL nuclear translocation in the absence of androgen [13, 19]. To investigate whether AR-Vs mitigate the inhibitory effect of AR-FL nuclear translocation by docetaxel, we expressed EGFP-AR-FL with or without TurboFP635-tagged AR-V7 or AR^{v567es} in the AR-null COS-7 cells. When co-expressed with TurboFP635, EGFP-AR-FL was retained in the cytoplasm following docetaxel treatment (Fig. 8A). However, in the presence of AR-V7-TurboFP635 or AR^{v567es}-TurboFP635, the inhibitory effect of docetaxel was significantly attenuated (Fig. 8A & 8B).

To further understand how AR-Vs circumvent docetaxel-mediated cytoplasmic sequestration of AR-FL, we conducted the microtubule-binding assay in COS-7 cells co-transfected with AR-FL and an AR-V. As shown in Fig. 8C, the binding of AR-FL to the microtubules was markedly reduced when it was co-expressed with AR-V7 or AR^{v567es}. Taken together, these results suggest that the constitutively active AR-V7 or AR^{v567es} could divert AR away from the microtubules, and facilitate its nuclear translocation in a microtubule-independent manner.

Nuclear import of AR-Vs is blocked by an importin β inhibitor

As an initial attempt to elucidate the nuclear translocation mechanisms of AR-V7 and AR^{v567es}, we investigated the involvement of the importin α/β machinery. FRAP assay was conducted in COS-7 transfected with EGFP-AR-V7 and treated with importazole, a specific inhibitor of importin β [31] . As shown by Fig. 9A & 9B, treatment with importazole

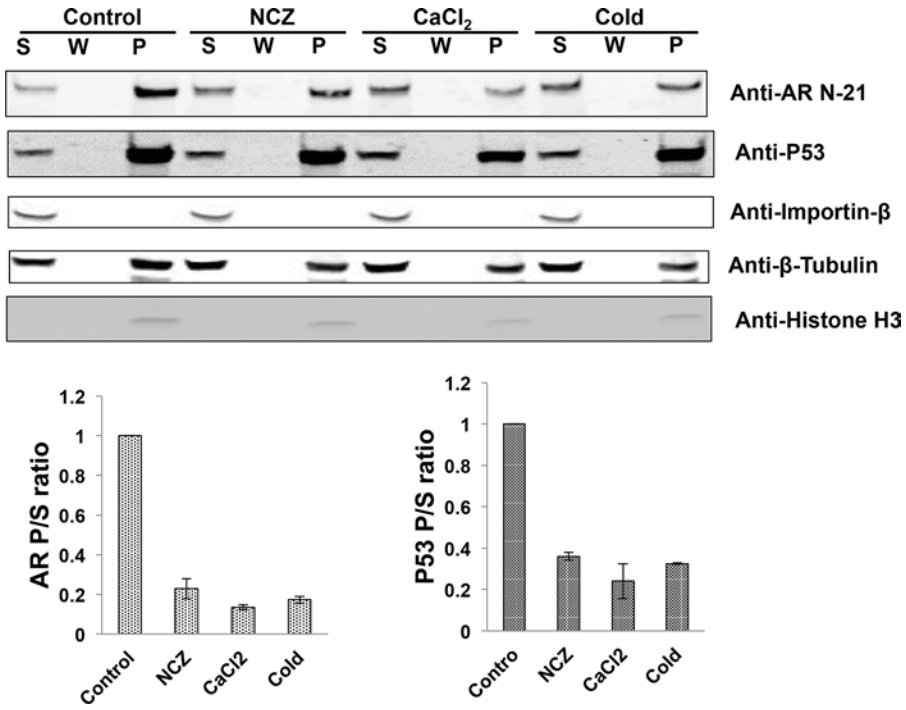

Figure 5: The full-length AR associates with the microtubules. COS-7 cells were transfected with an expression vector for AR-FL and *in vivo* microtubule binding assay was performed with a commercial kit (Cytoskeleton, BK038). Nocodazole (NCZ), $CaCl_2$, and low temperature (cold) were used to disrupt microtubule integrity. Assembled microtubules were precipitated by ultracentrifugation and the pellet was resuspended and analyzed by Western blot (Top). Importin β and p53 were used as negative and positive controls, respectively, and histone H3 was used to detect nuclear contamination. P, pellet; W, wash; S, supernatant. Bottom, the microtubule-binding activities for AR and p53 were quantitated by the P/S ratios. The results presented are mean ± SEM from three experiments.

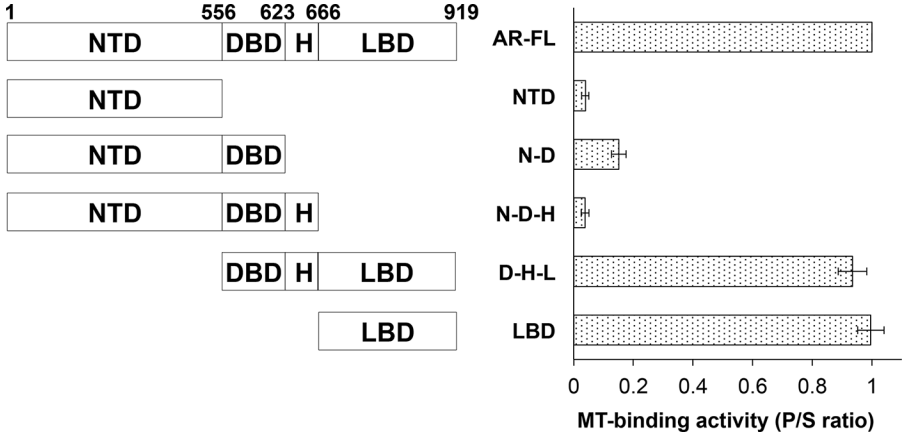

Figure 6: Microtubule-binding activity is mapped to the ligand-binding domain of AR. Left panel, a series of deletion constructs encompassing different domains of AR were generated and expressed in COS-7 cells. Right panel, the microtubule-binding activities of these constructs were analyzed by the *in vivo* microtubule binding assay and the Western blots (Supplementary Figure S5) were quantitated to calculate the P/S ratios. The results presented are mean ± SEM from three experiments. MT, microtubule.

significantly reduced the recovery of AR-V7 in the nucleus. Consistently, AR-V7 was found to accumulate in the cytoplasm following importazole treatment (Fig. 9C). FRAP assay showed a similar inhibition by importazole on the nuclear recovery of TurboFP635-tagged AR^{v567es} (Fig. 9D & 9E), suggesting that both variants are imported to the nucleus by the importin α/β machinery.

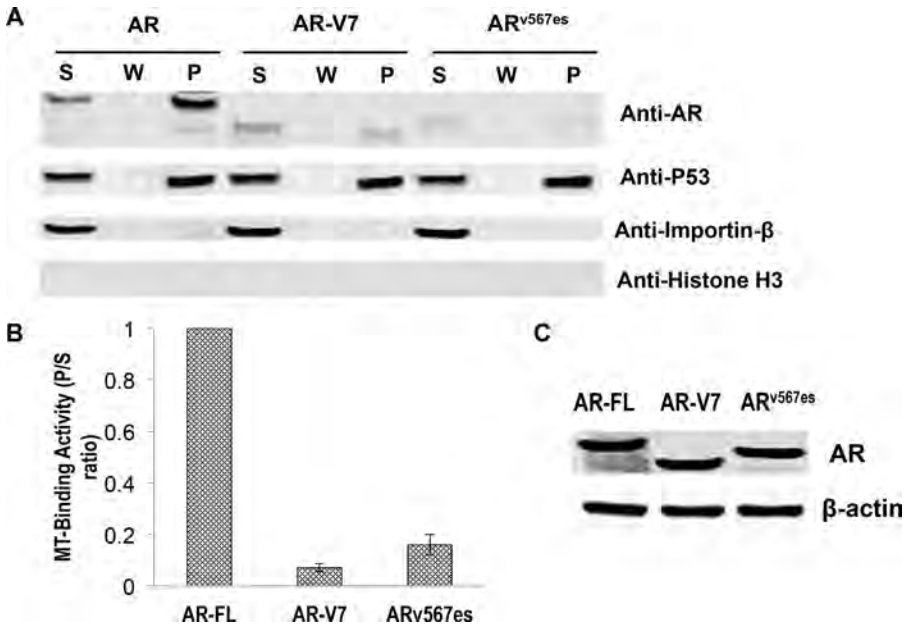

Figure 7: Poor microtubule-binding activities of the AR-Vs. COS-7 cells were transfected with an expression vector for AR-FL, AR-V7, and AR^{v567es} and cultured in an androgen-deprived condition. **A.** *In vivo* MT-binding assays. **B.** quantitation of the results in A. The results presented are mean ± SEM from three experiments. **C.** Western blot showing that the proteins were expressed at similar levels after transfection.

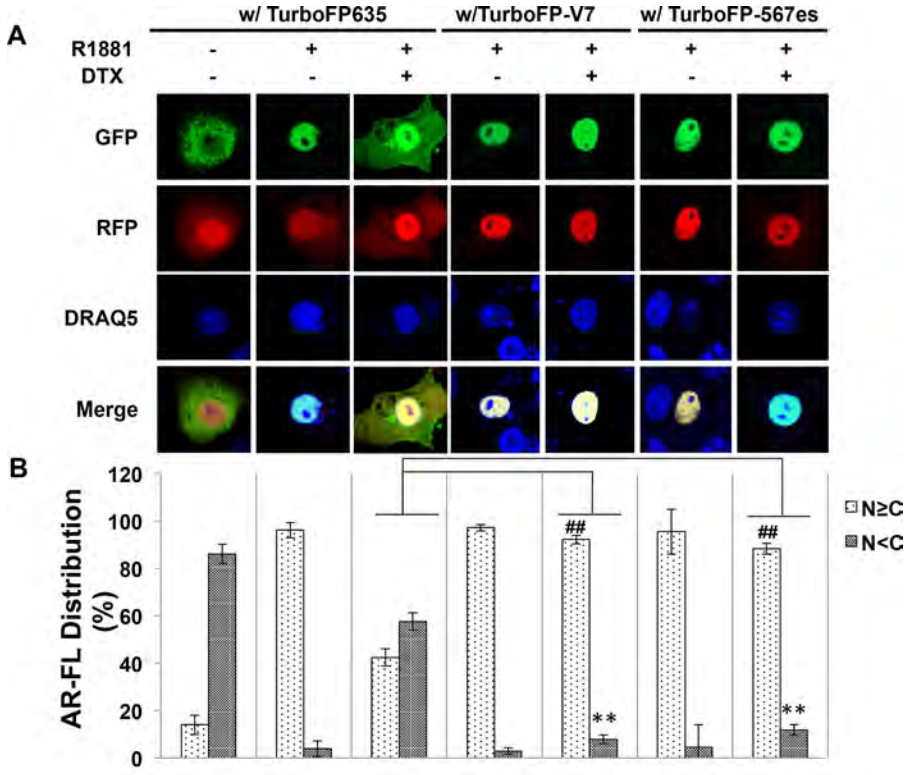

Figure 8: Cytoplasmic sequestration of AR-FL by docetaxel is attenuated by AR-V7 and AR^{v567es}. A. Confocal fluorescence microscopy of EGFP-AR-FL subcellular localization when it was expressed with TurboFP or with a TurboFP-tagged AR-V in COS-7 cells. **B.** Based on distribution of the green fluorescence signal, cells were categorized into cytoplasmic (N < C), or nuclear and equally nuclear and cytoplasmic (N ≥ C).% of cells in each category were quantified. DRAQ5 was used to stain the nuclei. Cells cultured in an androgen-deprived condition were pre-treated with 10 nM docetaxel for 6 hr, followed by treatment with 1 nM R1881 for 4 hr. ** and ## $P < 0.01$.

(*continued*)

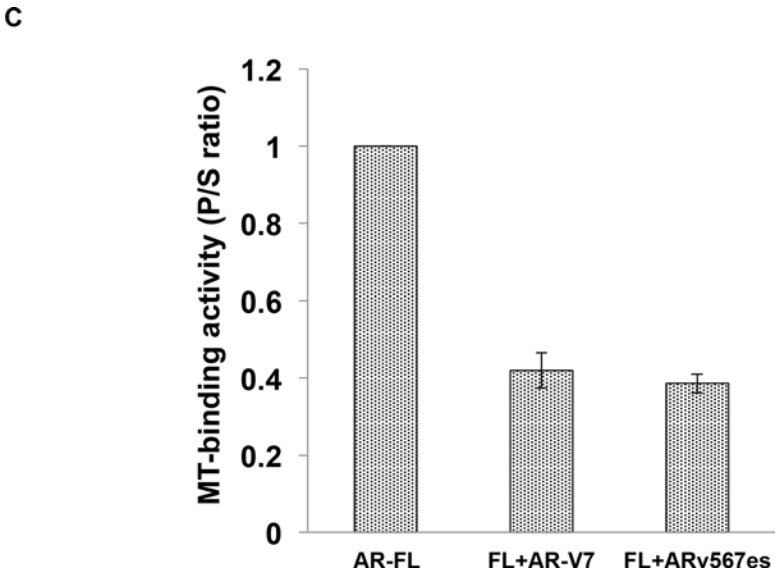

Figure 8: C. (*Continued*) *In vivo* MT-binding assay in COS-7 cells expressing AR-FL alone, or with AR-V7 or AR^{v567es}.

DISCUSSION

To date, docetaxel and cabazitaxel are the only chemotherapeutic agents that have been shown to offer survival benefits for patients with mCRPC. Even in today's rapidly evolving landscape of treatment options for mCRPC, taxane-based chemotherapy continues to be an important component of the treatment regimens. Recently, a randomized phase III trial supports the expansion of the indications of taxanes to earlier disease stages. The CHARRTED trial demonstrated that the addition of docetaxel to ADT in patients with high-volume, metastatic, hormonal-sensitive disease improves overall survival by 17 months (49.2 vs 32.2, $P = 0.0013$) than ADT alone [32]. With taxane chemotherapy projected to remain a mainstay in the treatment of prostate cancer, it is imperative to derive a better understanding of the mechanisms underlying the inherent and acquired taxane resistances, both of which are commonly observed in the clinic.

Resistance to taxanes could be multifactorial, involving general mechanisms of chemoresistance as well as mechanisms intrinsic to prostate cancer [33]. Existing literature focuses primarily on mechanisms common to many cancer types, including unfavorable tumor microenvironment, expression of drug efflux proteins, alterations in microtubule structure and/or function, expression of anti-apoptotic and cytoprotective proteins [34]. However, mechanisms that are specific to prostate cancer remain poorly understood. Recent clinical observations provided evidence for a cross-resistance of CRPC to hormonal therapy and taxane-based chemotherapy [21–25], suggesting a common culprit may underlie such a cross-resistance phenotype.

Our study represents a step forward in this direction. Herein, we present evidence that expression of constitutively active AR-Vs, but not over-expression of the canonical full-length receptor, protects prostate cancer cells from the cytotoxic effects of taxanes. We further show that taxane treatment selectively inhibits androgen-induced nuclear translocation and transactivation activity of AR-FL, while exerting no such inhibitory effects on the AR-Vs. These results reveal a fundamental difference in the nuclear translocation mechanisms of AR-FL and AR-Vs. AR-FL, as shown by this and other studies, utilizes a microtubule-facilitated pathway for nuclear translocation. This trafficking mechanism is shared by several nuclear proteins including glucocorticoid receptor (GR), p53, Rb, and parathyroid hormone-related protein (PTHrP) [29]. On the other hand, the nuclear import of AR-V7 and AR^{v567es} is not mediated by the microtubule pathway. The independence of the microtubule pathway enables the variants to evade taxane-induced cytoplasmic retention. Finally, we show that sequestration of AR-FL in the cytoplasm by taxanes is alleviated when AR-V7 or AR^{v567es} is present. This is likely caused by AR-V steering AR-FL away from the microtubules, as shown by reduced binding to the microtubules when AR-Vs are co-expressed. As an initial attempt to unveil the nuclear translocation mechanisms of the AR-Vs, we found that nuclear import of AR-V7 and AR^{v567es} is possibly mediated by the importin α/β machinery. Elucidation of the upstream events will likely lead to opportunities to design novel strategies to target this variant.

The clinical relevance of AR-Vs has been demonstrated by a myriad of studies. Higher expression of AR-V7 in hormone-naïve prostate tumors predicts increased risk of biochemical recurrence following radical

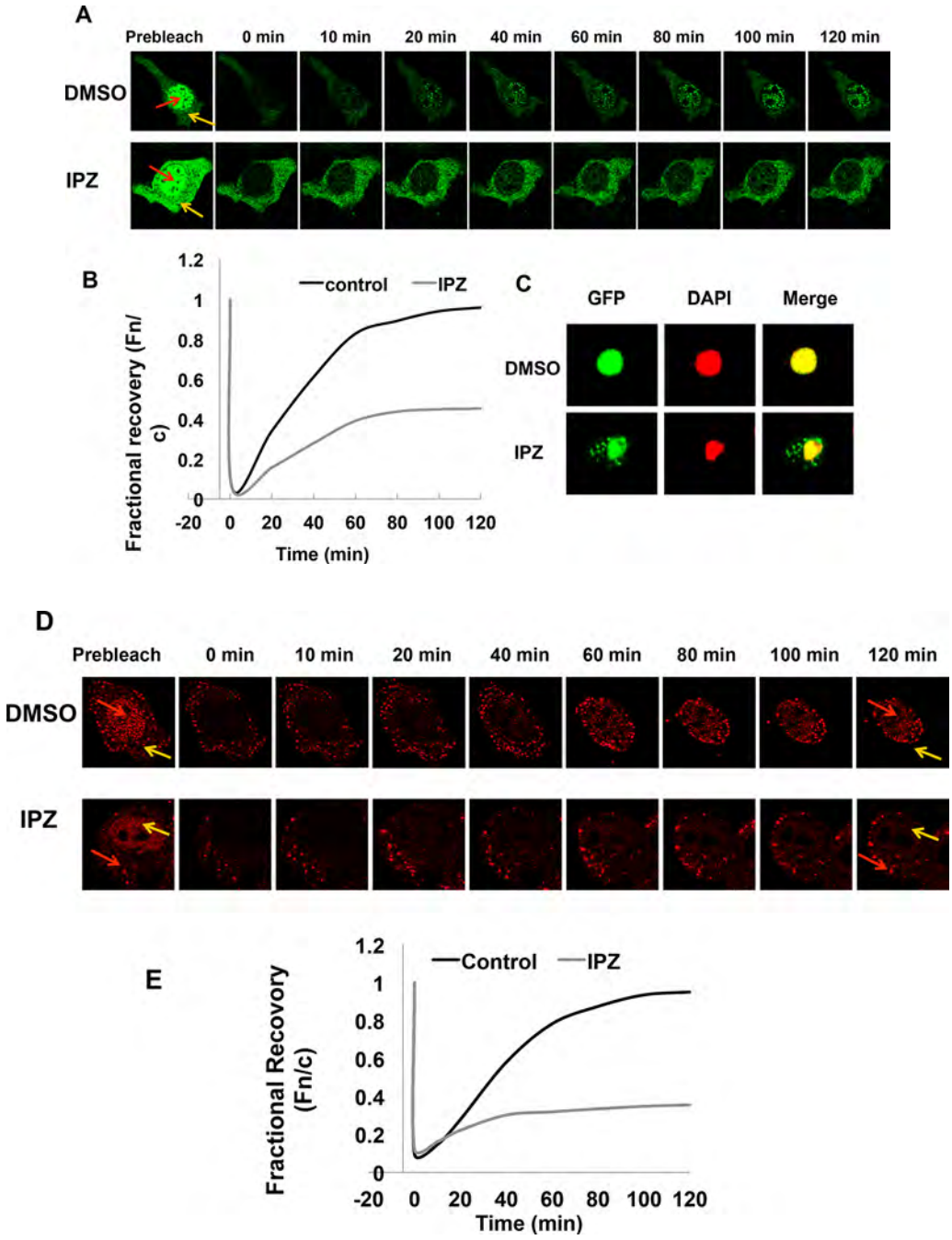

Figure 9: Nuclear translocation of AR-Vs is importin β-dependent. A. FRAP assays were performed in COS-7 cells expressing EGFP-tagged AR-V7. Cells were treated with DMSO or 50 μM importazole (IPZ) for 2 h before photobleaching. Confocal images taken at different intervals after photobleaching of the nuclei. Red and yellow arrows indicate nucleus and cytoplasm, respectively. **B.** Fn/c recovery plot for EGFP-AR-V7. **C.** COS-7 cells transfected with pEGFP-AR-V7 were treated with DMSO or 10 μM importazole for 48 h. DAPI was used for staining the nuclei. **D.** & **E.** confocal images (D) and Fn/c recovery plot (E) of FRAP assays in COS-7 cells expressing TurboFP635-tagged AR^{v567es} and treated with IPZ.

prostatectomy [11, 12], and patients with high levels of expression of AR-V7 or detectable expression of AR^{v567es} have a significantly shorter survival than other CRPC patients [15], indicating an association between AR-Vs expression and a more lethal form of prostate cancer. Studies have indicated that AR-Vs play important roles in resistance to androgen-directed therapies [17–19]. Particularly, a recent groundbreaking study by Antonarakis et al. showed that

patients positive for AR-V7 expression in circulating tumor cells have significantly worse responses to enzalutamide or abiraterone than AR-V7-negative patients [20].

While the roles of AR-Vs are well recognized in resistance to hormonal therapies, evidence has just started to accumulate to support their involvement in resistance to taxane chemotherapy. Thadani-Mulero and colleagues are the first to show evidence supporting a role of AR-V7 in resistance to taxane chemotherapy [35]. In addition, the study by Martin et al. [36] showed that in cells harboring AR-Vs, targeting the AR N-terminal domain of with a small molecule inhibitor enhances the therapeutic response to docetaxel [36]. A clinical study by Steinestel et al. showed expression of AR-V7 in circulating cancer cells significantly correlates with prior treatment with docetaxel [37]. Very recently, a clinical study presented at the American Society of Clinical Oncology Genitourinary Cancers Symposium investigated the responses to taxane chemotherapy in mCRPC patients with different AR-V7 status in circulating tumor cells [38]. Although all the clinical outcomes are worse in patients in the AR-V7(+) arm, the differences are not statistically significant [38]. The insignificant differences could result from the small sample size or due to a "threshold effect" of AR-V7. In other words, the influence of AR-V7 on taxane response may be manifested only when it is expressed above a certain level. Hence, the association of AR-Vs and sensitivity to taxane chemotherapy warrants further investigation in a larger cohort.

The main disparity between our study and that of Thadani-Mulero et al. [35] is on whether AR^{v567es} is inhibited by the taxanes. In contrast to the data present herein, Thadani-Mulero and colleagues showed that AR^{v567es} associates with the microtubules and that the nuclear translocation of AR^{v567es} is inhibited by taxanes. In addition, the microtubule-binding activity is mapped to the DNA-binding and hinge domains of AR [35]. One possible explanation for these discrepancies is the use of different assays. Thadani-Mulero et al. performed *in vitro* assays in which cell lysates containing AR proteins tagged by GFP or hemagglutinin were incubated with purified tubulin in a cell-free system to allow microtubule polymerization and association. In contrast, we conducted *in vivo* microtubule-binding assays in which the microtubules and associated proteins were extracted from cells expressing untagged AR isoforms. Another major difference between the two studies is the dosage of taxanes. Docetaxel was applied at a concentration of 1 μM in the cell culture studies by Thadani-Mulero et al., in contrast to the clinically attainable [39] nanomolar concentrations used in our studies. We demonstrated that treatment with taxanes, at the low nanomolar concentrations, fail to inhibit the transcriptional activity or nuclear import of AR^{v567es}.

The canonical AR nuclear localization signal (NLS) is located in the hinge domain, encoded by exons 3 and 4. Sequence analysis predicted that this NLS is truncated in AR-V7. However, the study by Chan et al. demonstrated that splicing of exon 3 with cryptic exon 3 in AR-V7 reconstitutes this bipartite NLS, which mediates the nuclear import of AR-V7 [40]. In addition, expression of a dominant negative mutant of Ran protein (RanQ69L) which causes premature dissociation of the importin/cargo complex, reduced nuclear localization of AR-V7 and AR^{v567es}. These findings are consistent with our importazole data, suggesting that the nuclear import of the AR-Vs is mediated by the importin α/β pathway. They also found that unlike AR-FL, the nuclear localization of AR-V7 and AR^{v567es} is not affected by an inhibitor for heat shock protein 90. Together, this study and our data present herein suggest a fundamental difference between AR-FL and AR-Vs in the events upstream of importin α/β-mediated nuclear entry.

In summary, our study provides support for the involvement of AR-V7 and AR^{v567es} in attenuating the response to taxane-based chemotherapy. Mechanistically, we demonstrated that both variants translocate to the nucleus in a microtubule-independent manner. Additionally, these variants can reduce the microtubule-binding activity of AR-FL, thus circumventing its cytoplasm sequestration triggered by taxanes. These findings have important clinical implications. The expression status of these AR variants could potentially be used as a biomarker to aid treatment selection and sequencing. More importantly, targeting AR-Vs could be a fruitful direction to pursue to enhance the efficacy of taxane chemotherapy. To this end, several small molecule inhibitors at various stages of clinical development have shown promises against AR-Vs [41–43], opening doors for novel therapeutic strategies.

MATERIALS AND METHODS

Cell lines and reagents

LNCaP, 22Rv1, and COS-7 cells were obtained from American Type Culture Collection. With the exception of drug-resistant lines, cells used in this study were within 20 passages (~3 months of non-continuous culturing). All cell lines were tested and authenticated by the method of short tandem repeat profiling. Docetaxel, cabazitaxel, and paclitaxel were purchased from Selleck Chemicals (Houston, TX). Nocodazole was from Sigma Aldrich, and KX-01 was provided by Kinex Pharmaceuticals. The following antibodies were used in Western blot analysis: anti-GAPDH, anti-AR (N-terminus-directed, PG-21; Millipore), anti-importin β1, anti-β-actin (Santa Cruz), anti-p53 (Calbiochem), anti-histone H3 (Cell Signaling), and anti-AR-V7 (Precision Antibody).

Selection of taxane resistant cell lines

22Rv1 cells were initially treated with 10 nM paclitaxel for 72 hours and the surviving cells were re-seeded and allowed to recover for 1 week.

Paclitaxel-resistant cells were developed over a period of 2 months by stepwise increasing concentrations of paclitaxel (5–50 nM). Age-matched parental cells which did not receive treatments were maintained in parallel. Docetaxel-resistant 22Rv1 and LNCaP95 lines were generated in a similar manner, but with different doses of docetaxel (5 nM initially, 2.5–20 nM for selection). The resistant cells were continuously maintained in the highest concentration of the taxane in which they selected.

Western blotting

Cells were washed with ice-cold phosphate-buffered saline (PBS) and lysed with 2X Cell Lysis Buffer (Cell Signaling) containing a phosphatase inhibitor and the protease inhibitor cocktail (Sigma). After incubating the cells on ice for 30 min, lysates were collected by centrifugation at 10, 000 rpm for 10 minutes. Protein concentrations were determined by the BCA Protein Assay kit (Pierce). The samples were separated on 10% SDS-polyacrylamide gels and transferred onto polyvinylidene fluoride (PVDF) membranes. After blocking in TBS buffer (150 mM NaCl, 10 mM Tris, pH 7.4) containing 5% nonfat milk, the blots were incubated with a primary antibody overnight at 4°C and a fluorescent-labeled secondary antibody for 1 h at room temperature. The fluorescent signals were obtained by the Odyssey Infrared Imaging System (LI-COR Bioscience).

Transient transfection and reporter gene assay

COS-7 cells were seeded in 10-cm dishes at a density to reach 80–90% confluency at time of transfection. Transient transfection was performed by using the Lipofectamine and Plus reagents following the manufacturer's instructions (Invitrogen). Cells were co-transfected with ARR3-luc luciferase reporter contruct and pRL-TK, along with a plasmid encoding for AR-FL, AR-V7 or AR^{v567es}. After incubating with the transfection mixture for 4 h, cells were re-plated in RPMI 1640 containing 10% charcoal-stripped fetal bovine serum (cs-FBS). Cells were allowed to recover overnight before treated with DTX (1 and 2.5 nM) or PTX (2.5 or 5 nM) in the presence or absence of 10 nM DHT. Dual-luciferase assay was performed at 24 h post treatment using the Dual-luciferase Reporter Assay System (Promega). The renilla luciferase activity was used to normalize that of firefly luciferase.

Confocal fluorescence microscopy

Subcellular localization of AR proteins was analyzed by confocal fluorescence microscopy. The pTurboFP635-AR-V7 and pTurboFP635-AR^{v567es} plasmids were generated by cloning the cDNA fragments for AR-V7 and AR^{v567es}, respectively, into the pCMV-TurboFP635 vector. COS-7 cells were transfected with indicated plasmids and cultured in phenol red-free RPMI-1640 supplemented with 10% cs-FBS. At 40 hr after transfection, cells were pre-treated with or without 10 nM docetaxel for 6 hr, followed by treatment with or without 1 nM R1881 for 4 hr. COS-7 cells were subsequently fixed with 2% paraformaldehyde, and the nuclei were stained with 2.5 μM DRAQ5 (Cell Signaling). Confocal images were obtained by using a Leica TCS SP2 system with a 63X oil-immersion objective on a Z-stage, and an average of 6 fields with ~10 cells per field were captured for each group. Data quantitation was performed as described [44].

Fluorescence recovery after photobleaching (FRAP) assay

FRAP assay was performed using a Leica TCS SP2 microscope equipped with 20X, 40X and 63X oil immersion lenses (Nikon) in combination with a heated stage (Delta T Open Dish System, Bioptechs), as described by Roth et al. [45] with modifications. Briefly, three images were obtained before photobleaching using 10% of total laser power with excitation at 488 nm, scanning at a rate of 8 μs/pixel. Photobleaching was performed by scanning an area covering the entire nucleus 10 times at a rate of 12.5 μs/pixel, applying 100% of the laser power. After bleaching, the recovery of fluorescence was monitored by scanning the cells at 1 minute intervals for up to 2 hours, using detector and laser settings identical to those prior to photobleaching. Image analysis was carried out by using the NIH Image J Software to quantitate the nuclear (Fn) and cytoplasmic (Fc) fluorescence signals. The ratios of Fn to Fc (Fn/c) were calculated and the extent of recovery was determined by fractional recovery of Fn/c, which is the Fn/c at each time point divided by the prebleach Fn/c. The data were fitted exponentially to generate the fractional recovery plot.

In vivo microtubule binding assay

The AR deletion constructs were generated by inserting PCR products of the corresponding cDNA regions into the pcDNA3.1(-) vector. The resulting plasmids were sequenced to confirm sequence accuracy and in-frame reading. COS-7 cells were transfected with indicated plasmids and cultured in RPMI 1640 medium supplemented with 10% cs-FBS. Microtubule-binding assay was performed by using the Microtubule/Tubulin *In Vivo* Assay Kit (Cytoskeleton Inc., Cat.# BK038) following the manufacturer's instructions. Briefly, 3×10^6 cells were lysed in 4 mL pre-warmed (37°C) Lysis and Microtubule Stabilization 2 (LMS2) buffer (100 mM PIPES, pH 6.9, 5 mM $MgCl_2$, 1mM EGTA, 30% (v/v) glycerol, 0.1% Nonidet P40, 0.1% Triton X-100, 0.1% Tween 20, 0.1% β-mercaptoethanol, 0.001% Antifoam, 100 μM GTP, 1 mM ATP, 1 × protease inhibitors cocktail) in a 10-cm cell culture dish. The lysates were collected

and spun at 2,000 g for 10 min at 37°C to remove nuclei and unbroken cells. The supernatants were then subjected to ultracentrifugation at 100, 000 g for 30 min at 37°C to separate the microtubules from the soluble, unpolymerized tubulin. The pellet was washed with pre-warmed LMS2 buffer and centrifuged at 100, 000 g for 30 min at 37°C. For microtubule destabilization conditions, LMS2 buffer containing nocodazole (5 μg/ml) or $CaCl_2$ (2 mM), or ice-cold LMS2 buffer were used in the above procedure. The pellets were resuspended in ice-cold 2 mM $CaCl_2$ and incubated in room temperature for 15 min to depolymerize microtubules. The supernatant (S), wash solution (W), and resuspended pellet (P) were adjusted to equal volumes and analyzed by Western blotting.

Statistical analysis

Statistical analysis was performed using Microsoft Excel. The *Student's* two-tailed *t*-test was used to determine the difference in means between two groups. $P < 0.05$ is considered significant. Data are presented as mean ± standard error of men (SEM).

ACKNOWLEDGMENTS

We are indebted to Dr. Yun Qiu for providing the AR-FL and AR-V7 cDNA constructs, to Dr. Stephen R. Plymate for the AR^{v567es} cDNA construct, to Dr. Jun Luo for the EGFP-AR-FL and EGFP-AR-V7 expression vectors, and to Dr. Rebecca Heald for providing importazole.

GRANT SUPPORT

This work was supported by the following grants: ACS RSG-07-218-01-TBE, DOD W81XWH-12-1-0275 and W81XWH-14-1-0480, NIH/NCI R01CA188609, Louisiana Board of Regents LEQSF(2012-15)-RD-A-25, NIH/NIGMS 5P20GM103518-10, Louisiana Cancer Research Consortium Fund, Oliver Sartor Prostate Cancer Research Fund, National Natural Science Foundation of China Projects 81272851 and 81430087.

CONFLICTS OF INTEREST

No conflicts of interest to declare.

REFERENCES

1. Harris WP, Mostaghel EA, Nelson PS, Montgomery B. Androgen deprivation therapy: progress in understanding mechanisms of resistance and optimizing androgen depletion. Nat Clin Pract Urol. 2009; 6:76–85.
2. Tannock IF, de WR, Berry WR, Horti J, Pluzanska A, Chi KN, Oudard S, Theodore C, James ND, Turesson I, Rosenthal MA, Eisenberger MA. Docetaxel plus prednisone or mitoxantrone plus prednisone for advanced prostate cancer. N Engl J Med. 2004; 351:1502–1512.
3. De Bono JS, Oudard S, Ozguroglu M, Hansen S, Machiels JP, Kocak I, Gravis G, Bodrogi I, Mackenzie MJ, Shen L, Roessner M, Gupta S, Sartor AO. Prednisone plus cabazitaxel or mitoxantrone for metastatic castration-resistant prostate cancer progressing after docetaxel treatment: a randomised open-label trial. Lancet. 2010; 376:1147–1154.
4. De Bono JS, Logothetis CJ, Molina A, Fizazi K, North S, Chu L, Chi KN, Jones RJ, Goodman OB, Saad F, Staffurth JN, Mainwaring P, Harland S, Flaig TW, Hutson TE, Cheng T, Patterson H, Hainsworth JD, Ryan CJ, Sternberg CN, Ellard SL, Flechon A, Saleh M, Scholz M, Efstathiou E, Zivi A, Bianchini D, Loriot Y, Chieffo N, Kheoh T, Haqq CM, Scher HI. Abiraterone and increased survival in metastatic prostate cancer. N Engl J Med. 2011; 364:1995–2005.
5. Scher HI, Fizazi K, Saad F, Taplin M-E, Sternberg CN, Miller K, de Wit R, Mulders P, Chi KN, Shore ND, Armstrong AJ, Flaig TW, Fléchon A, Mainwaring P, Fleming M, Hainsworth JD, Hirmand M, Selby B, Seely L, de Bono JS. Increased survival with enzalutamide in prostate cancer after chemotherapy. N Engl J Med. 2012; 367:1187–1197.
6. Jordan MA, Wilson L. Microtubules as a target for anticancer drugs. Nat Rev Cancer. 2004; 4:253–265.
7. Zhu ML, Horbinski CM, Garzotto M, Qian DZ, Beer TM, Kyprianou N. Tubulin-targeting chemotherapy impairs androgen receptor activity in prostate cancer. Cancer Res. 2010; 70:7992–8002.
8. Darshan MS, Loftus MS, Thadani-Mulero M, Levy BP, Escuin D, Zhou XK, Gjyrezi A, Chanel-Vos C, Shen R, Tagawa ST, Bander NH, Nanus DM, Giannakakou P. Taxane-induced blockade to nuclear accumulation of the androgen receptor predicts clinical responses in metastatic prostate cancer. Cancer Res. 2011; 71:6019–6029.
9. Gan L, Chen S, Wang Y, Watahiki A, Bohrer L, Sun Z, Wang Y, Huang H. Inhibition of the androgen receptor as a novel mechanism of taxol chemotherapy in prostate cancer. Cancer Res. 2009; 69:8386–8394.
10. Dehm SM, Schmidt LJ, Heemers HV, Vessella RL, Tindall DJ. Splicing of a novel androgen receptor exon generates a constitutively active androgen receptor that mediates prostate cancer therapy resistance. Cancer Res. 2008; 68:5469–5477.
11. Hu R, Dunn TA, Wei S, Isharwal S, Veltri RW, Humphreys E, Han M, Partin AW, Vessella RL, Isaacs WB, Bova GS, Luo J. Ligand-independent androgen receptor variants derived from splicing of cryptic exons signify hormone-refractory prostate cancer. Cancer Res. 2009; 69:16–22.
12. Guo Z, Yang X, Sun F, Jiang R, Linn DE, Chen H, Chen H, Kong X, Melamed J, Tepper CG, Kung HJ, Brodie AM, Edwards J, Qiu Y. A novel androgen receptor splice variant

is up-regulated during prostate cancer progression and promotes androgen depletion-resistant growth. Cancer Res. 2009; 69:2305–2313.

13. Sun S, Sprenger CC, Vessella RL, Haugk K, Soriano K, Mostaghel EA, Page ST, Coleman IM, Nguyen HM, Sun H, Nelson PS, Plymate SR. Castration resistance in human prostate cancer is conferred by a frequently occurring androgen receptor splice variant. J Clin Invest. 2010; 120:2715–2730.
14. Hu R, Lu C, Mostaghel EA, Yegnasubramanian S, Gurel M, Tannahill C, Edwards J, Isaacs WB, Nelson PS, Bluemn E, Plymate SR, Luo J. Distinct transcriptional programs mediated by the ligand-dependent full-length androgen receptor and its splice variants in castration-resistant prostate cancer. Cancer Res. 2012; 72:3457–3462.
15. Hornberg E, Ylitalo EB, Crnalic S, Antti H, Stattin P, Widmark A, Bergh A, Wikstrom P. Expression of androgen receptor splice variants in prostate cancer bone metastases is associated with castration-resistance and short survival. PLoS One. 2011; 6:e19059.
16. Zhang X, Morrissey C, Sun S, Ketchandji M, Nelson PS, True LD, Vakar-Lopez F, Vessella RL, Plymate SR. Androgen receptor variants cccur frequently in castration resistant prostate cancer metastases. PLoS ONE. 2011; 6:e27970.
17. Mostaghel EA, Marck BT, Plymate SR, Vessella RL, Balk S, Matsumoto AM, Nelson PS, Montgomery RB. Resistance to CYPA1 inhibition with abiraterone in castration-resistant prostate cancer: induction of steroidogenesis and androgen receptor splice variants. Clin Cancer Res. 2011; 17:5913–5925.
18. Li Y, Chan SC, Brand LJ, Hwang TH, Silverstein KAT, Dehm SM. Androgen receptor splice variants mediate enzalutamide resistance in castration-resistant prostate cancer Cell Lines. Cancer Res. 2013; 73:483–489.
19. Cao B, Qi Y, Zhang G, Xu D, Zhan Y, Alvarez X, Guo Z, Fu X, Plymate SR, Sartor O, Zhang H, Dong Y. Androgen receptor splice variants activating the full-length receptor in mediating resistance to androgen-directed therapy. Oncotarget. 2014; 5:1646–1656.
20. Antonarakis ES, Lu C, Wang H, Luber B, Nakazawa M, Roeser JC, Chen Y, Mohammad TA, Chen Y, Fedor HL, Lotan TL, Zheng Q, De Marzo AM, Isaacs JT, Isaacs WB, Nadal R, Paller CJ, Denmeade SR, Carducci MA, Eisenberger MA, Luo J. AR-V7 and resistance to enzalutamide and abiraterone in prostate cancer. N Engl J Med. 2014; 371:1028–1038.
21. Mezynski J, Pezaro C, Bianchini D, Zivi A, Sandhu S, Thompson E, Hunt J, Sheridan E, Baikady B, Sarvadikar A, Maier G, Reid AHM, Mulick Cassidy A, Olmos D, Attard G, de Bono J. Antitumour activity of docetaxel following treatment with the CYP17A1 inhibitor abiraterone: clinical evidence for cross-resistance? Ann Oncol Off J Eur Soc Med Oncol ESMO. 2012; 23:2943–2947.
22. Schweizer MT, Zhou XC, Wang H, Bassi S, Carducci MA, Eisenberger MA, Antonarakis ES. The influence of prior abiraterone treatment on the clinical activity of docetaxel in men with metastatic castration-resistant prostate cancer. Eur Urol. 2014; 66:646–652.
23. Van Soest RJ, van Royen ME, de Morrée ES, Moll JM, Teubel W, Wiemer EAC, Mathijssen RHJ, de Wit R, van Weerden WM. Cross-resistance between taxanes and new hormonal agents abiraterone and enzalutamide may affect drug sequence choices in metastatic castration-resistant prostate cancer. Eur J Cancer. 2013; 49:3821–3830.
24. Nadal R, Zhang Z, Rahman H, Schweizer MT, Denmeade SR, Paller CJ, Carducci MA, Eisenberger MA, Antonarakis ES. Clinical activity of enzalutamide in docetaxel-naïve and docetaxel-pretreated patients with metastatic castration-resistant prostate cancer. The Prostate. 2014; 74:1560–1568.
25. Cheng HH, Gulati R, Azad A, Nadal R, Twardowski P, Vaishampayan UN, Agarwal N, Heath EI, Pal SK, Rehman HT, Leiter A, Batten JA, Montgomery RB, Galsky MD, Antonarakis ES, Chi KN, Yu EY. Activity of enzalutamide in men with metastatic castration-resistant prostate cancer is affected by prior treatment with abiraterone and/or docetaxel. Prostate Cancer Prostatic Dis. 2015; 18:122–127.
26. Anbalagan M, Ali A, Jones RK, Marsden CG, Sheng M, Carrier L, Bu Y, Hangauer D, Rowan BG. Peptidomimetic Src/pretubulin inhibitor KX-01 alone and in combination with paclitaxel suppresses growth, metastasis in human ER/PR/HER2-negative tumor xenografts. Mol Cancer Ther. 2012; 11:1936–1947.
27. Cassimeris LU, Wadsworth P, Salmon ED. Dynamics of microtubule depolymerization in monocytes. J Cell Biol. 1986; 102:2023–2032.
28. Roth DM, Moseley GW, Glover D, Pouton CW, Jans DA. A microtubule-facilitated nuclear import pathway for cancer regulatory proteins. Traffic. 2007; 8:673–686.
29. Roth DM, Moseley GW, Pouton CW, Jans DA. Mechanism of microtubule-facilitated “fast track” nuclear import. J Biol Chem. 2011; 286:14335–14351.
30. Giannakakou P, Sackett DL, Ward Y, Webster KR, Blagosklonny MV, Fojo T. p53 is associated with cellular microtubules and is transported to the nucleus by dynein. Nat Cell Biol. 2000; 2:709–717.
31. Soderholm JF, Bird SL, Kalab P, Sampathkumar Y, Hasegawa K, Uehara-Bingen M, Weis K, Heald R. Importazole, a small molecule inhibitor of the transport receptor importin-β. ACS Chem Biol. 2011; 6:700–708.
32. Sweeney C, Chen Y-H, Carducci MA, Liu G, Jarrard DF, Eisenberger MA, Wong Y-N, Hahn NM, Kohli M, Vogelzang NJ, Cooney MM, Dreicer R, Picus J, Shevrin DH, Hussain M, Garcia JA, DiPaola RS. Impact on overall survival (OS) with chemohormonal therapy versus hormonal therapy for hormone-sensitive newly

metastatic prostate cancer (mPrCa): An ECOG-led phase III randomized trial. J Clin Oncol. 2014; 32:5s.

33. Seruga B, Ocana A, Tannock IF. Drug resistance in metastatic castration-resistant prostate cancer. Nat Rev Clin Oncol. 2011; 8:12–23.

34. Antonarakis ES, Armstrong AJ. Evolving standards in the treatment of docetaxel-refractory castration-resistant prostate cancer. Prostate Cancer Prostatic Dis. 2011; 14:192–205.

35. Thadani-Mulero M, Portella L, Sun S, Sung M, Matov A, Vessella RL, Corey E, Nanus DM, Plymate SR, Giannakakou P. Androgen receptor splice variants determine taxane sensitivity in prostate cancer. Cancer Res. 2014; 74:2270–2282.

36. Martin SK, Banuelos CA, Sadar MD, Kyprianou N. N-terminal targeting of androgen receptor variant enhances response of castration resistant prostate cancer to taxane chemotherapy. Mol Oncol. 2015; 9:628–639.

37. Steinestel J, Luedeke M, Arndt A, Schnoeller TJ, Lennerz JK, Wurm C, Maier C, Cronauer MV, Steinestel K, Schrader AJ. Detecting predictive androgen receptor modifications in circulating prostate cancer cells. Oncotarget. . Published online Apr 23, 2015.

38. Antonarakis ES, Lu C, Chen Y, Luber B, Wang H, Nakazawa M, Marzo AMD, Isaacs WB, Nadal R, Paller CJ, Denmeade SR, Carducci MA, Eisenberger MA, Luo J. AR splice variant 7 (AR-V7) and response to taxanes in men with metastatic castration-resistant prostate cancer (mCRPC). J Clin Oncol. 2015; 33 .

39. Clarke SJ, Rivory LP. Clinical pharmacokinetics of docetaxel. Clin Pharmacokinet. 1999; 36:99–114.

40. Chan SC, Li Y, Dehm SM. Androgen receptor splice variants activate androgen receptor target genes and support aberrant prostate cancer cell growth independent of canonical androgen receptor nuclear localization signal. J Biol Chem. 2012; 287:19736–19749.

41. Andersen RJ, Mawji NR, Wang J, Wang G, Haile S, Myung JK, Watt K, Tam T, Yang YC, Banuelos CA, Williams DE, McEwan IJ, Wang Y, Sadar MD. Regression of castrate-recurrent prostate cancer by a small-molecule inhibitor of the amino-terminus domain of the androgen receptor. Cancer Cell. 2010; 17:535–546.

42. Liu C, Lou W, Zhu Y, Nadiminty N, Schwartz CT, Evans CP, Gao AC. Niclosamide inhibits androgen receptor variants expression and overcomes enzalutamide resistance in castration-resistant prostate cancer. Clin Cancer Res. 2014; 20:3198–3210.

43. Purushottamachar P, Godbole AM, Gediya LK, Martin MS, Vasaitis TS, Kwegyir-Afful AK, Ramalingam S, Ates-Alagoz Z, Njar VCO. Systematic structure modifications of multi-target prostate cancer drug candidate galeterone to produce novel androgen receptor down-regulating agents as an approach to treatment of advanced prostate cancer. J Med Chem. 2013; 56:4880–4898.

44. Li J, Cao B, Liu X, Fu X, Xiong Z, Chen L, Sartor O, Dong Y, Zhang H. Berberine suppresses androgen receptor signaling in prostate cancer. Mol Cancer Ther. 2011; 10:1346–1356.

45. Roth DM, Harper I, Pouton CW, Jans DA. Modulation of nucleocytoplasmic trafficking by retention in cytoplasm or nucleus. J Cell Biochem. 2009; 107:1160–1167.

Published OnlineFirst June 9, 2015; DOI: 10.1158/0008-5472.CAN-15-0381

Tumor and Stem Cell Biology

Cancer Research

Androgen Receptor Splice Variants Dimerize to Transactivate Target Genes

Duo Xu[1,2,3], Yang Zhan[2], Yanfeng Qi[2], Bo Cao[1,2], Shanshan Bai[1,2], Wei Xu[4], Sanjiv S. Gambhir[5], Peng Lee[6], Oliver Sartor[7,8], Erik K. Flemington[9], Haitao Zhang[9], Chang-Deng Hu[10], and Yan Dong[1,2,11]

Abstract

Constitutively active androgen receptor splice variants (AR-V) lacking the ligand-binding domain have been implicated in the pathogenesis of castration-resistant prostate cancer and in mediating resistance to newer drugs that target the androgen axis. AR-V regulates expression of both canonical AR targets and a unique set of cancer-specific targets that are enriched for cell-cycle functions. However, little is known about how AR-V controls gene expression. Here, we report that two major AR-Vs, termed AR-V7 and AR^{v567es}, not only homodimerize and heterodimerize with each other but also heterodimerize with full-length androgen receptor (AR-FL) in an androgen-independent manner. We found that heterodimerization of AR-V and AR-FL was mediated by N- and C-terminal interactions and by the DNA-binding domain of each molecule, whereas AR-V homodimerization was mediated only by DNA-binding domain interactions. Notably, AR-V dimerization was required to transactivate target genes and to confer castration-resistant cell growth. Our results clarify the mechanism by which AR-Vs mediate gene regulation and provide a pivotal pathway for rational drug design to disrupt AR-V signaling as a rational strategy for the effective treatment of advanced prostate cancer. *Cancer Res; 75(17); 3663–71. ©2015 AACR.*

Introduction

Recurrence with lethal castration-resistant prostate cancer (CRPC) after androgen deprivation therapy remains the major challenge in treatment of advanced prostate cancer (1, 2). Significant advances in our understanding of continued androgen receptor (AR) signaling in CRPC have led to the development and FDA approval of two next-generation androgen-directed therapies, the androgen biosynthesis inhibitor abiraterone and the potent AR antagonist enzalutamide (3, 4). These drugs heralded a new era of prostate cancer therapy. However, some patients present with therapy-resistant disease, and most initial responders develop acquired resistance within months of therapy initiation (3, 4). The resistance is typically accompanied by increased prostate-specific antigen (PSA), indicating reactivated AR signaling (3, 4). Accumulating evidences indicate that prostate tumors can adapt to these androgen-directed therapies, including abiraterone and enzalutamide, by signaling through constitutively active alternative splicing variants of AR (AR-V; refs. 5–17).

To date, 15 AR-Vs have been identified (18). Structurally, AR-Vs have insertions of cryptic exons downstream of the exons encoding the DNA-binding domain (DBD) or deletions of the exons encoding the ligand-binding domain (LBD), resulting in a disrupted AR open reading frame and expression of LBD-truncated AR (6, 7, 9, 15, 19, 20). Because the N-terminal domain, which contains the most critical transactivation domain of the receptor (AF1), and the DBD remain intact in the majority of the AR-Vs, many AR-Vs display ligand-independent transactivation. AR-V7 (aka AR3) and AR^{v567es} (aka AR-V12) are two major AR-Vs expressed in clinical specimens (7–10, 15, 17). They localize primarily to the nucleus, activate target gene expression in a ligand-independent manner, and promote castration-resistant growth of prostate cancer cells both *in vitro* and *in vivo* (7, 9, 15, 19–21). Strikingly, patients with high levels of expression of AR-V7 or detectable expression of AR^{v567es} in prostate tumors have a shorter survival than other CRPC patients (8). Moreover, AR-V7 expression in circulating tumor cells of CRPC patients is associated with resistance to both abiraterone and enzalutamide (17). These findings indicate an association between AR-V expression and a more lethal form of prostate cancer, and also highlight the importance of AR-Vs in limiting the efficacy of androgen-directed therapies.

[1]College of Life Sciences, Jilin University, Changchun, China. [2]Department of Structural and Cellular Biology, Tulane University School of Medicine, Tulane Cancer Center, New Orleans, Louisiana. [3]School of Nursing, Jilin University, Changchun, China. [4]McArdle Laboratory for Cancer Research, University of Wisconsin, Madison, Wisconsin. [5]Bio-X Program and Department of Radiology, Stanford University School of Medicine, Stanford, California. [6]Department of Pathology, New York University School of Medicine, New York, New York. [7]Department of Urology, Tulane University School of Medicine, Tulane Cancer Center, New Orleans, Louisiana. [8]Department of Medicine, Tulane University School of Medicine, Tulane Cancer Center, New Orleans, Louisiana. [9]Department of Pathology and Laboratory Medicine, Tulane University School of Medicine, Tulane Cancer Center, New Orleans, Louisiana. [10]Department of Medicinal Chemistry and Molecular Pharmacology, Purdue University, West Lafayette, Indiana. [11]National Engineering Laboratory for AIDS Vaccine, Jilin University, Changchun, China.

Note: Supplementary data for this article are available at Cancer Research Online (http://cancerres.aacrjournals.org/).

D. Xu and Y. Zhan contributed equally to this article.

Corresponding Author: Yan Dong, Tulane University School of Medicine, 1430 Tulane Avenue SL-49, New Orleans, LA 70112. Phone: 504-988-4761; Fax: 504-988-0468; E-mail: ydong@tulane.edu

doi: 10.1158/0008-5472.CAN-15-0381

Published OnlineFirst June 9, 2015; DOI: 10.1158/0008-5472.CAN-15-0381

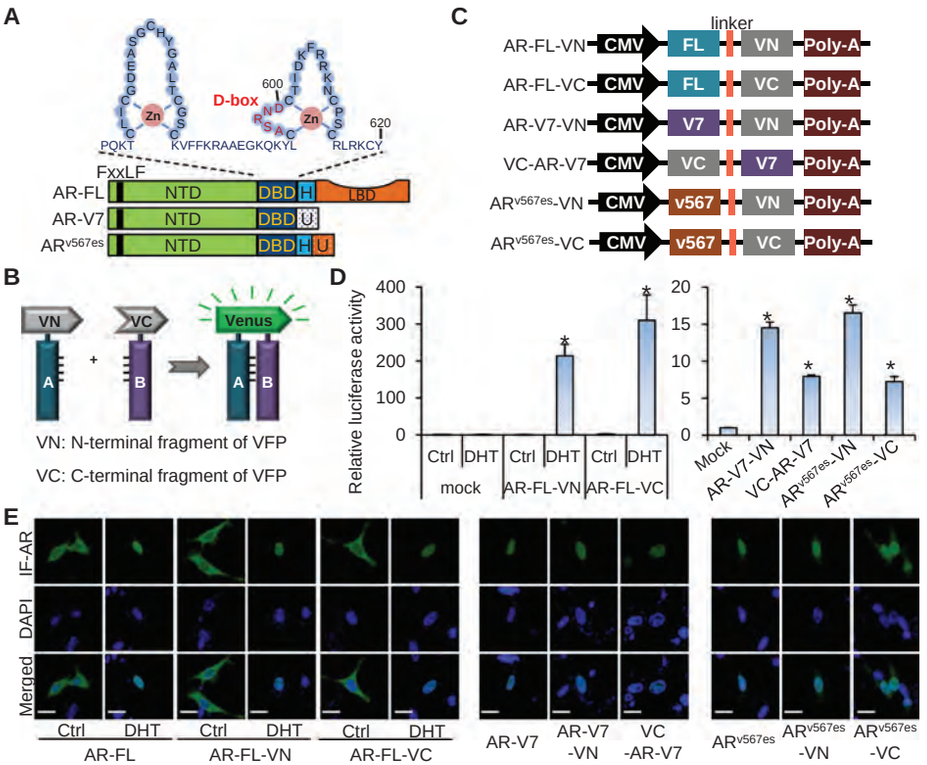

Figure 1.
AR-FL and AR-Vs in BiFC fusion proteins are functional. A, schematic representation of AR-FL, AR-V7, and AR^{v567es} protein structure. The DBD is composed of two zinc fingers. NTD, N-terminal domain; H, hinge region; U, unique C-terminal sequence. D-box and FxxLF motif mediate AR-FL dimerization. B, a schematic of the principle of the BiFC assay. VFP, Venus fluorescent protein. C, schematic diagram of the constructs used in the BiFC assay. D, luciferase assay showing AR transactivating activity in PC-3 cells cotransfected with the indicated BiFC construct and the ARE-luc plasmid. *, $P < 0.05$ from mock control. E, immunofluorescent (IF) staining showing protein fusion does not change subcellular localization of AR-FL, AR-V7, or AR^{v567es}. The indicated expression construct or BiFC fusion construct was transfected into PC-3 cells, and immunofluorescent staining was conducted at 48 hours after transfection. DAPI, nuclear stain. Scale bars, 10 μm. Cells were cultured under androgen-deprived condition unless specified. DHT, 1 nmol/L for 24 hours.

AR-V7 and AR^{v567es} can regulate the expression of both canonical AR targets and a unique set of targets enriched for cell-cycle function independent of the full-length AR (AR-FL; refs. 7, 10, 15). AR-V7 and AR^{v567es} can also activate AR-FL in the absence of androgen by facilitating AR-FL nuclear localization and coregulate the expression of canonical AR targets (5). It has long been appreciated that dimerization is required for AR-FL to regulate target gene expression (22), but little is known about AR-V dimerization. Coimmunoprecipitation of endogenous AR^{v567es} and AR-FL (15) and co-occupancy of the PSA promoter by AR-V7 and AR-FL (5) suggest that AR-Vs may form heterodimers with AR-FL. However, whether AR-Vs homodimerize or heterodimerize with each other and whether the dimerization is required for AR-Vs to regulate target genes and to confer castration-resistant cell growth are currently unknown.

Dimerization of AR-FL is mediated mainly through N/C-terminal interactions, via the FxxLF motif in the N-terminal domain and the coactivator groove in the LBD, and DBD/DBD interactions, via the dimerization box (D-box; ref. 22). Because the FxxLF motif and the D-box (Fig. 1A) are maintained in the majority of the AR-Vs identified, we hypothesize that these AR-Vs can form heterodimers with each other as well as homodimers via DBD/DBD interactions and that they can also form heterodimers with AR-FL via DBD/DBD and N/C interactions. In the current study, we tested this hypothesis by using the bimolecular fluorescence complementation (BiFC) and bioluminescence resonance energy transfer (BRET) assays, which have complementary capabilities for characterizing protein–protein interactions in live cells. BiFC allows direct visualization of subcellular locations of the interactions (23), while BRET allows real-time detection of complex formation (24, 25).

Materials and Methods

Cell lines and reagents

LNCaP, PC-3, DU145, VCaP, and HEK-293T cells were obtained from the ATCC, and cultured as described (26). C4-2 was provided by Dr. Shahriar Koochekpour (Roswell Park Cancer Institute, Buffalo, NY). All the cell lines were authenticated on April 1, 2015 by the method of short tandem repeat profiling at the Genetica DNA Laboratories. Enzalutamide was purchased from Selleck Chemicals.

Plasmid construction

To generate different BiFC fusion constructs of AR-FL, AR-V7, and AR^{v567es}, we PCR amplified the AR-FL, AR-V7, and AR^{v567es} cDNAs from their respective expression construct, and cloned the PCR amplicons separately into a TA-cloning vector (Promega). Fusion constructs of AR-FL, AR^{v567es}, and AR-V7 with either VN or VC were generated by subcloning the cDNAs from the TA plasmids into the SalI and XhoI sites of the pBiFC-VN155 and pBiFC-VC155 vectors. The mutant BiFC-AR-V and BiFC-AR-FL constructs with mutations at the FxxLF motif (F23,27A/L26A) and/or D-box (A596T/S597T) were generated by site-directed mutagenesis by using the Q5 site-Directed Mutagenesis Kit (New England BioLabs). BRET-fusion constructs of AR-FL, AR-V7, and AR^{v567es} were generated by subcloning the AR-FL, AR-V7, and AR^{v567es} cDNA from the respective TA plasmids into the BamHI and XbaI sites of the pcDNA3.1-RLuc8.6 and TurboFP635 vectors (24). The doxycycline-inducible AR^{v567es} lentiviral construct was generated by subcloning the AR^{v567es} cDNA from its TA plasmid first into the pDONR221 vector (Invitrogen) and subsequently into the doxycycline-inducible pHAGE-Ind-EF1a-DEST-GH lentiviral construct

Published OnlineFirst June 9, 2015; DOI: 10.1158/0008-5472.CAN-15-0381

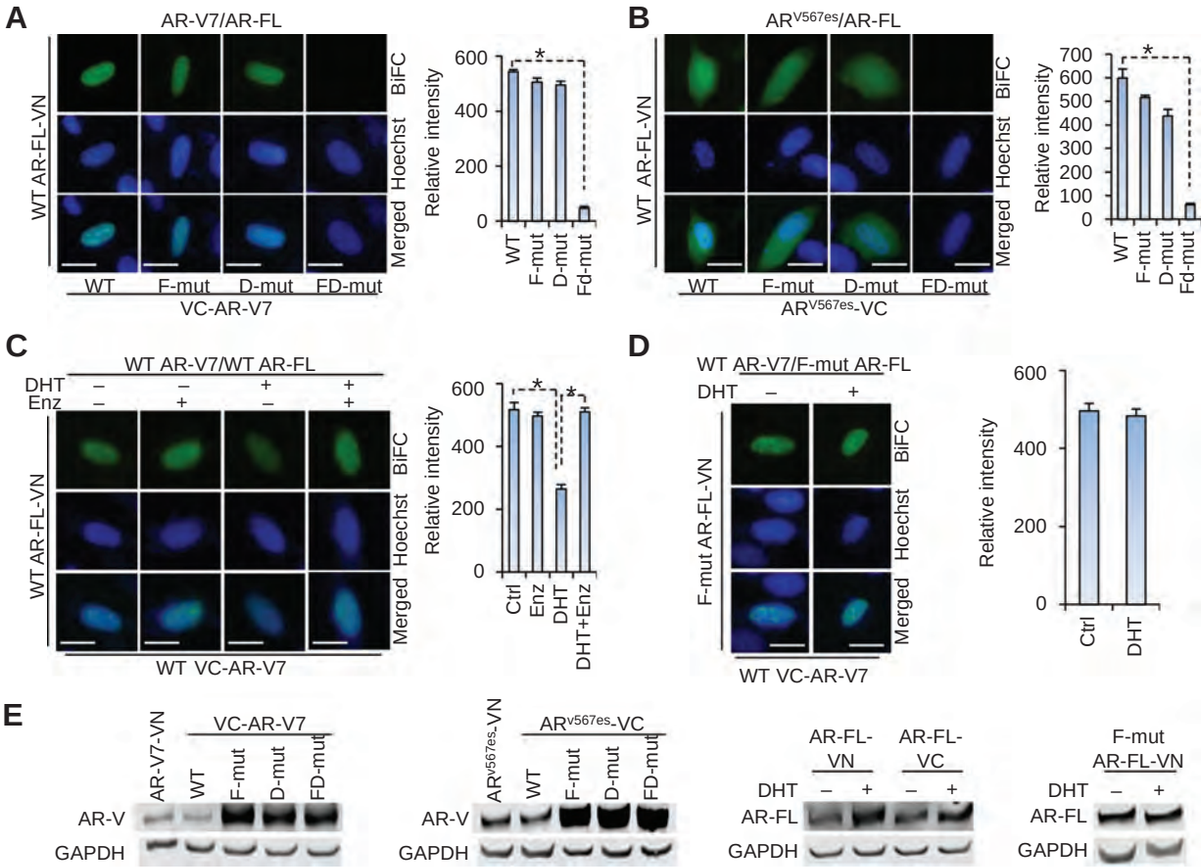

Figure 2.
AR-V7 and AR^{v567es} heterodimerize with AR-FL through both N/C and DBD/DBD interactions. wt, wild-type; F-mut, FxxLF-motif mutant; D-mut, D-box mutant; FD-mut, FxxLF-motif and D-Box double mutant. Hoechst, nuclear stain. Scale bars, 10 μm. *, $P < 0.05$. A and B, dimerization was detected by the BiFC assay in PC-3 cells under androgen-deprived condition. Right, quantitation of BiFC signals by flow cytometry. C and D, pretreatment with androgen attenuates the dimerization between AR-V7 and wt AR-FL (C) but not the dimerization between AR-V7 and F-mut AR-FL (D). PC-3 cells were treated with 1 nmol/L DHT with or without 10 μmol/L enzalutamide (Enz) right after transfection with the indicated BiFC constructs, and BiFC signal was assessed at 48 hours after transfection. Right, quantitation of BiFC signals by flow cytometry. E, Western blotting with a pan-AR antibody showing expression of the BiFC-fusion proteins. Individual fusion construct was transfected into PC-3 cells cultured under androgen-deprived condition unless specified. DHT, 1 nmol/L for 24 hours.

by using the Gateway Cloning System (Invitrogen). All plasmids were sequence verified.

DNA transfection and reporter gene assay

PC-3 and HEK-293T cells were transfected by using the TransIT-2020 (Mirus Bio LLC) and TurboFect reagents (Thermo Scientific), respectively, per instruction of the manufacturer. DU145, C4-2, and LNCaP cells were transfected by using the Lipofectamine 2000 and Plus reagent (Invitrogen) as described (27). Reporter gene assay was performed as previously described (28) with either an androgen-responsive element-luciferase plasmid (ARE-luc) containing three ARE regions ligated in tandem to the luciferase reporter or a luciferase construct driven by three repeats of an AR-V–specific promoter element of the ubiquitin-conjugating enzyme E2C (UBE2C) gene (UBE2C-luc). To ensure an even transfection efficiency, we conducted the transfection in bulk and then split the transfected cells for luciferase assay.

Immunofluorescence staining

Cells were transfected with indicated plasmids on Poly-D-Lysine–coated coverslips (neuVitro) and cultured in phenol red–free medium supplemented with 10% charcoal-stripped FBS. For the dihydrotestosterone (DHT) groups, 1 nmol/L DHT was added at 24 hours after transfection. At 48 hours after transfection, cells were fixed with 70% ethanol, and incubated with a pan-AR antibody (PG-21, Millipore; 1:200) overnight at 4°C and subsequently with Alexa Fluor 488–conjugated secondary antibody (Invitrogen; 1:1,000) for 1 hour at room temperature in the dark. Nuclei were then stained with 4′,6-diamidino-2-phenylindole (DAPI). Confocal images were obtained by using a Leica TCS SP2 system with a 40× oil-immersion objective on a Z-stage.

BiFC analysis

Cells were cotransfected with different BiFC fusion constructs. At 48 hours after transfection, cells were incubated with Hoechst33342 (Invitrogen) and observed by fluorescence microscopy (Olympus). For flow cytometry quantitation of BiFC signals, the pDsRed2-C1 construct (Clontech) was cotransfected with the BiFC fusion constructs. At 48 hours after transfection, cells were trypsinized, and the Venus and DsRed fluorescence were analyzed by flow cytometry.

Published OnlineFirst June 9, 2015; DOI: 10.1158/0008-5472.CAN-15-0381

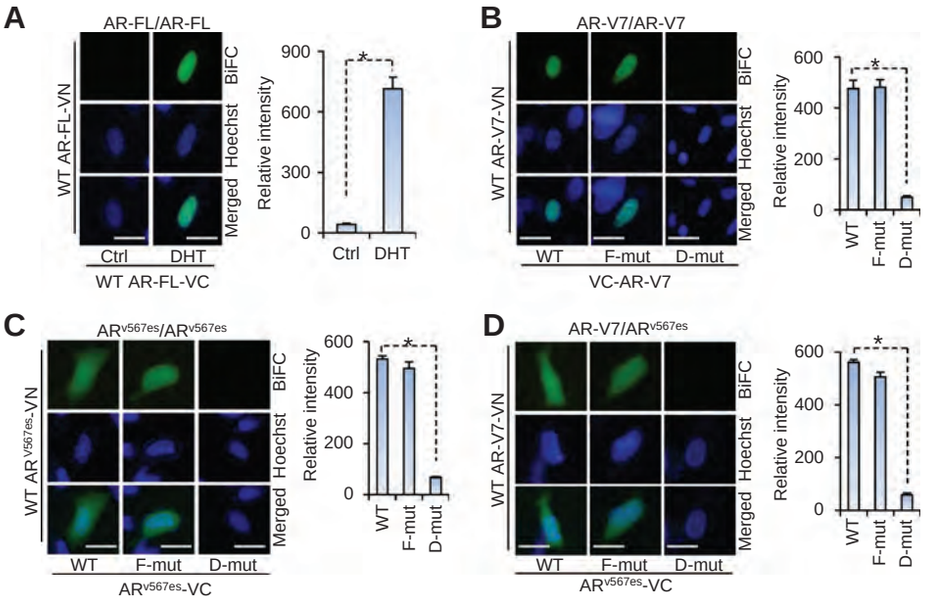

Figure 3.
AR-V and AR-V dimerize through DBD/DBD interactions. AR-FL homodimerization (A), AR-V7 homodimerization (B), AR^{v567es} homodimerization (C), and AR-V7/AR^{v567es} heterodimerization (D) were detected by BiFC assay in PC-3 cells under androgen-deprived condition unless specified. DHT, 1 nmol/L for 24 hours. Right panels, quantitation of BiFC signals by flow cytometry. wt, wild-type; F-mut, FxxLF-motif mutant; D-mut, D-box mutant. Hoechst, nuclear stain. Scale bars, 10 μm. *, $P < 0.05$. In contrast to AR-FL/AR-FL and AR-V7/AR-V7 dimerization, which were detected mainly in the nucleus (>90%), AR^{v567es}/AR^{v567es} and AR-V7/AR^{v567es} dimerization were observed in both the nucleus (37% and 57%, respectively) and the cytoplasm (63% and 43%, respectively).

Western blot analysis

The procedure was described previously (29). The anti-GAPDH (Millipore), anti-AR (N-20, Santa Cruz Biotechnology), anti-HSP70 (Abcam), anti-Turbo-red fluorescent protein (Abcam), and anti-*Renilla*-luciferase (Thermo Scientific) antibodies were used.

Quantitative RT-PCR and cell growth assay

Quantitative RT-PCR (qRT-PCR) was performed as described (30), and the qPCR primer probe sets were from IDT. Cell growth was determined by the sulforhodamine (SRB) assay as described (31). To ensure an even transduction efficiency, we conducted the transduction of the cells with packaged lentivirus in bulk, and then split the transduced cells for qRT-PCR and SRB assays.

BRET assay

Cells were either transfected with an RLuc BRET fusion plasmid or cotransfected with an RLuc and a TFP BRET fusion plasmid. At 72 hours after transfection, cells were detached with 5 mmol/L EDTA in PBS and resuspended in PBS with 1% sucrose. Cells were counted and seeded in triplicate into a 96-well white-wall microplate at 10^5 cells per well. Freshly prepared coelenterazine (Nanolight Technology) in water was added to the cells at a final concentration of 25 μmol/L. BRET readings at 528 nm and 635 nm were obtained immediately with a Synergy 2 microplate reader (BioTek). The BRET ratio was calculated by subtracting the ratio of 635-nm emission and 528-nm emission obtained from cells coexpressing the RLuc and TFP fusion proteins from the background BRET ratio resulting from cells expressing the RLuc fusion protein alone in the same experiment: BRET ratio = (emission at 635 nm)/(emission at 528 nm) − (emission at 635 nm RLuc only)/(emission at 528 nm RLuc only).

Statistical analysis

The Student two-tailed *t* test was used to determine the mean differences between two groups. $P < 0.05$ is considered significant. Data are presented as mean ± SEM.

Results

Characterization of AR-FL and AR-Vs in BiFC fusion proteins

For BiFC analysis of interaction between proteins A and B, the two proteins are fused separately to either the N- or C-terminal fragment of the Venus fluorescent protein (VN or VC, Fig. 1B). If the two proteins dimerize, the interaction allows regeneration of the Venus fluorescent protein to emit fluorescent signal (23). Because BiFC depends on the relative orientation of the fusion proteins (23), we generated all possible combinations of N- and C-terminal fusions by cloning the AR-FL, AR^{v567es}, or AR-V7 cDNA either in front of or after VN or VC. Different pairs of fusion protein constructs were transfected into the AR-null PC-3 cells (to avoid confounding effect of endogenous AR), and the fusion protein constructs exhibiting the highest BiFC signals (Fig. 1C) were chosen for further analysis. The transactivating abilities of the fusion proteins were tested by the reporter gene assay. Although the protein fusion affected the relative activities of the fusion proteins (Figs. 1D and Supplementary Fig. S1), all the fusion proteins can transactivate target genes. Immunofluorescence assay further showed that the AR-FL and AR-Vs in the fusion proteins have the same subcellular localizations as the respective nonfusion AR isoform (Fig. 1E). Collectively, the data indicated that AR-FL and AR-Vs are functional in the fusion proteins.

BiFC detection of AR-V/AR-FL heterodimerization

To assess the ability of AR-V7 and AR^{v567es} to heterodimerize with AR-FL, we cotransfected the AR-V- and AR-FL BiFC fusion constructs into PC-3 cells and quantitated the Venus fluorescence signal by flow cytometry. Both AR-V7 and AR^{v567es} dimerized with AR-FL, and the dimerization did not require androgen (Fig. 2A and B). To delineate the dimerization interface, we generated mutant BiFC-AR-V constructs with mutations at the FxxLF motif (F23,27A/L26A) and/or D-box (A596T/S597T). FxxLF motif and D-box mediate AR-FL homodimerization through N/C and DBD/DBD interactions, respectively (22). Only mutating both motifs abolished AR-V/AR-FL dimerization (Fig. 2A and B), indicating that both N/C and DBD/DBD interactions mediate

Published OnlineFirst June 9, 2015; DOI: 10.1158/0008-5472.CAN-15-0381

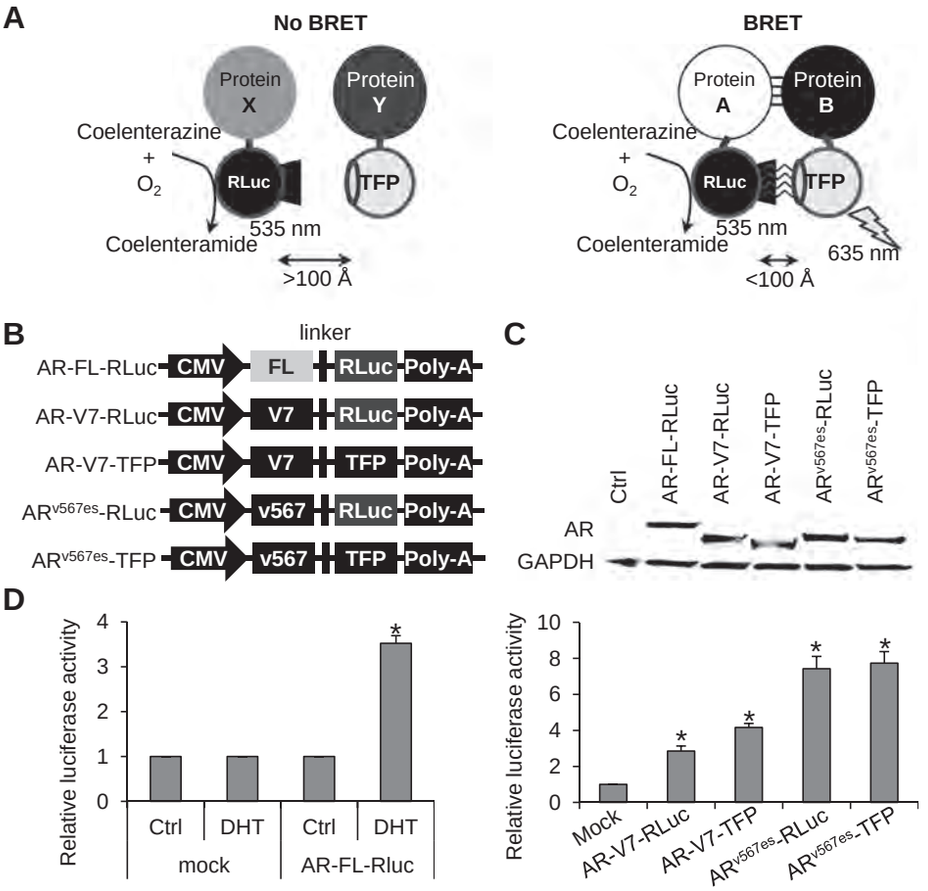

Figure 4.
AR-FL and AR-Vs in BRET fusion proteins are functional. A, a schematic of the principle of the BRET assay. B, schematic diagram of the constructs used in the BRET assay. RLuc, RLuc8.6 luciferase; TFP, TurboFP635 fluorescent protein. C, Western blotting with a pan-AR antibody showing expression of the BRET-fusion proteins. Individual fusion construct was transfected into HEK-293T cells cultured under androgen-deprived condition. D, luciferase assay showing AR *trans*-activating activity in HEK-293T cells cotransfected with the indicated BRET construct and the ARE-luc plasmid. Cells were cultured under androgen-deprived condition unless specified. DHT, 1 nmol/L for 24 hours. *, $P < 0.05$ from mock control.

the dimerization. Mutating one motif did not lead to significant change of BiFC signal (Fig. 2A and B), likely due to compensation of the loss of one mode of interaction by the other. Similar results were obtained in DU145 and HEK-293T cells (Supplementary Figs. S2 and S3). Intriguingly, although AR^{v567es}/AR-FL dimerization was observed in both the cytoplasm and the nucleus, AR-V7/AR-FL dimerization was detected primarily in the nucleus in the vast majority of the cells (Figs. 2A and B, Supplementary Figs. S2A, S2B, S3A, and S3B).

Pretreatment of cells with DHT attenuated AR-V7/AR-FL dimerization, and this effect was blocked by the antiandrogen enzalutamide (Fig. 2C). Conversely, DHT pretreatment produced minimal effect on the dimerization of AR-V7 and the FxxLF-motif–mutated AR-FL (Fig. 2D), which lost the ability to homodimerize upon androgen treatment (Supplementary Fig. S4B; ref. 32). These data indicate that AR-V7 may compete with AR-FL for dimerizing with AR-FL. Notably, the expression of each of the wild-type and mutant fusion proteins was confirmed by Western blotting (Fig. 2E). Collectively, our data demonstrated androgen-independent dimerization between AR-V and AR-FL, and indicated that AR-V/AR-FL dimerization may attenuate androgen induction of AR-FL homodimerization.

BiFC detection of AR-V/AR-V dimerization

We further showed that, like liganded AR-FL (Figs. 3A and Supplementary Fig. S4), both AR-Vs can form a homodimer when expressed alone (Figs. 3B and C and Supplementary Figs. S2C, S2D, S3C, and S3D). The homodimerization can also occur when AR-V is coexpressed with AR-FL and even when it is expressed at a much lower level than AR-FL (Supplementary Fig. S5). Moreover, AR-V7 and AR^{v567es} can heterodimerize (Fig. 3D). Mutating D-box, but not the FxxLF motif, abolished AR-V/AR-V interactions, indicating that AR-Vs homodimerize and heterodimerize with each other through DBD/DBD interactions. Interestingly, similar to AR-V7/AR-FL dimerization, AR-V7/AR-V7 dimerization was detected primarily in the nucleus (Figs. 3B and Supplementary Figs. S2C and S3C). However, AR^{v567es}/AR^{v567es} and AR-V7/AR^{v567es} dimerization were observed in both the nucleus and the cytoplasm (Fig. 3C and D and Supplementary Figs. S2D and S3D).

Characterization of AR-FL and AR-Vs in BRET fusion proteins

We then used the newest BRET system, BRET6 (24), to confirm the BiFC results. BRET6 is based on energy transfer between the Rluc8.6 *Renilla* luciferase (Rluc) energy donor and the turbo red fluorescent protein (TFP) energy acceptor when the donor and acceptor are brought into close proximity by their fused proteins (Fig. 4A). Similar to BiFC, BRET also depends on the relative orientation of the fusion proteins. We therefore generated all possible combinations of N- and C-terminal fusions by cloning the AR-FL, AR^{v567es}, or AR-V7 cDNA either in front of or after Rluc

Published OnlineFirst June 9, 2015; DOI: 10.1158/0008-5472.CAN-15-0381

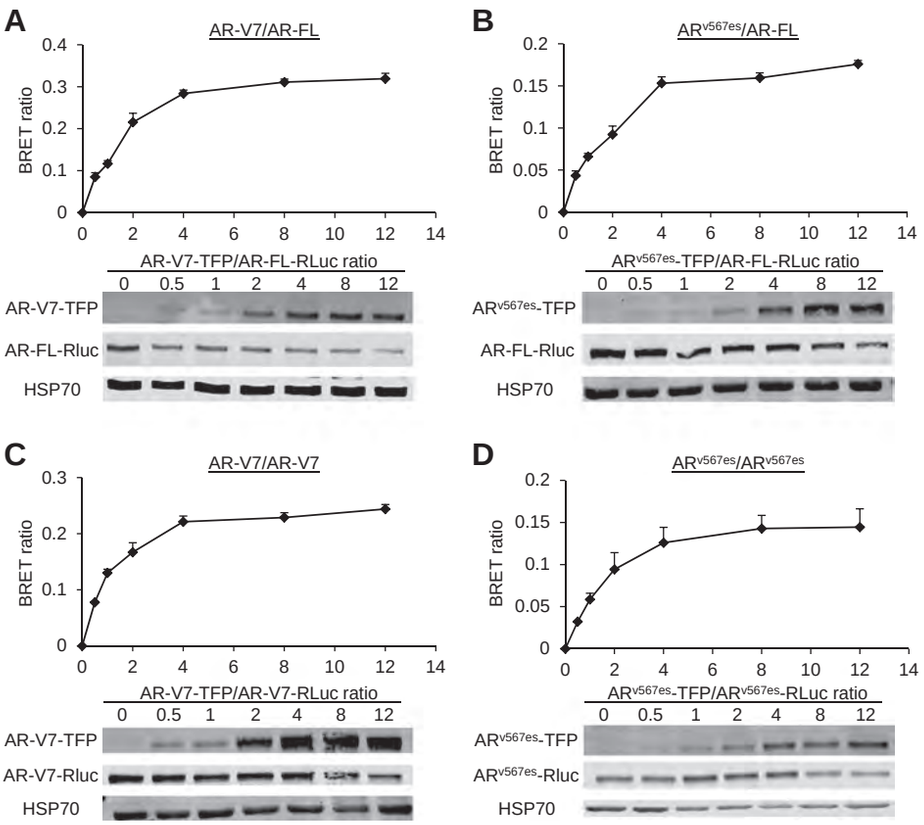

Figure 5.
BRET assay confirmation of AR-V/AR-FL and AR-V/AR-V dimerization. Indicated BRET fusion constructs were cotransfected into HEK-293T cells at different ratios, and BRET signal was measured after the addition of the coelenterazine substrate. Lower panels, Western blotting with an antibody against TFP, RLuc, or HSP70 showing the levels of the fusion proteins expressed. Cells were cultured under androgen-deprived condition.

or TFP. Different pairs of the fusion protein constructs were transfected into the AR-null HEK-293T cells (to avoid confounding effect of endogenous AR), and the fusion protein constructs exhibiting the highest BRET signals (Fig. 4B) were chosen for further analysis. The expression of these fusion proteins was confirmed by Western blotting (Fig. 4C). Furthermore, their abilities to transactivate were validated by luciferase assay with the cotransfection of the ARE-luc plasmid (Fig. 4D), indicating that AR-FL and AR-Vs are functional in the BRET fusion proteins.

BRET confirmation of AR-V/AR-FL and AR-V/AR-V dimerization

Figure 5 shows the BRET saturation curves for different combinations of the BRET fusion proteins in HEK-293T cells. The BRET ratios increased hyperbolically and rapidly saturated with the increase in the ratio of energy acceptor to energy donor, indicating specific protein–protein interaction (33). Similar to the BiFC data, mutating the FxxLF-motif and/or the D-box inhibited AR-V/AR-FL and AR-V/AR-V dimerization (Supplementary Fig. S6). Thus, the BRET data confirmed the BiFC results, showing the ability of AR-Vs to heterodimerize with AR-FL and to homodimerize. AR^{v567es}/AR^{v567es} interaction was further demonstrated by coimmunoprecipitation assay (Supplementary Fig. S7).

Dimerization is required for AR-V action

To assess the requirement of dimerization for AR-V action, we first performed reporter gene assay with the wild-type or the dimerization mutants of AR-V. As shown in Fig. 6A, the dimerization mutants completely lost the ability to transactivate, indicating a requirement of dimerization for AR-V transactivation. We then analyzed the ability of the wild-type and dimerization mutants of AR-Vs to regulate target gene expression and castration-resistant growth of prostate cancer cells. To this end, we infected the AR-FL–expressing LNCaP cells with lentivirus encoding AR-V7 or doxycycline-inducible AR^{v567es}. Mutation of the FxxLF motif alone or both the FxxLF motif and D-box attenuated AR-V induction of androgen-independent expression of the canonical AR target PSA and the AR-V–specific target UBE2C (Fig. 6B) as well as castration-resistant cell growth (Fig. 6C). The data indicated the requirement of dimerization for AR-Vs to regulate target genes and to confer castration-resistant cell growth.

Discussion

The current study represents the first to show the dimeric nature of AR-Vs in live cells. Using BiFC and BRET assays, we showed that AR-V7 and AR^{v567es} not only homodimerize and heterodimerize with each other but also heterodimerize with AR-FL. The dimerization does not require androgen. By mutating the FxxLF motif in the N-terminal domain and/or D-box in DBD of AR-Vs, we further showed that AR-V/AR-FL dimerization is mediated by both N/C and DBD/DBD interactions, whereas AR-V/AR-V dimerization is through DBD/DBD interactions. Because AR-Vs lack the C-terminal domain, the N/C interactions between AR-V and AR-FL is mediated presumably via the FxxLF motif of AR-V and the C-terminal domain of AR-FL. Significantly, dimerization mutants of AR-Vs lose the ability to transactivate target genes and to confer

Published OnlineFirst June 9, 2015; DOI: 10.1158/0008-5472.CAN-15-0381

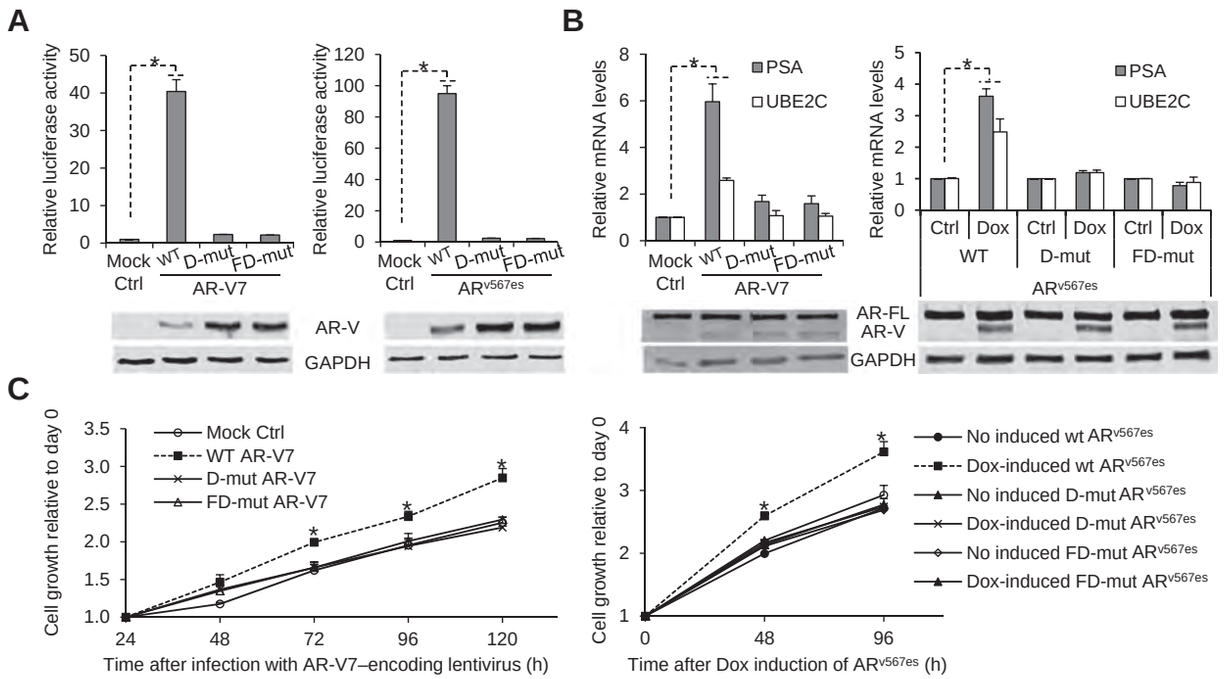

Figure 6.
Dimerization mutants of AR-Vs lose ability to transactivate and to promote castration-resistant cell growth. A, wild-type or dimerization mutant of AR-V was cotransfected with the ARE-luc plasmid, and cells were cultured under androgen-deprived condition. B and C, LNCaP cells were infected in bulk with lentivirus encoding wild-type or dimerization mutant of AR-V7 (left) or doxycycline-inducible wild-type or dimerization mutant of AR^{v567es} (right). At 24 hours after infection, cells were reseeded and treated with or without 200 ng/mL doxycycline and incubated for an additional 48 hours for qRT-PCR analysis of target genes (B) or for the indicated time for SRB assay of cell growth (C). Western blotting confirmed AR-V expression. *, $P < 0.05$ from control cells.

castration-resistant cell growth, indicating the requirement of dimerization for important functions of AR-Vs.

Our finding on AR-V/AR-FL interaction is in accordance with the previous reports on AR^{v567es} and AR-FL coimmunoprecipitation (15) as well as on AR-V7 and AR-FL co-occupancy of the PSA promoter (5), providing a direct evidence for their dimerization. Interestingly, we found that the androgen-independent dimerization between AR-V and AR-FL may mitigate androgen induction of AR-FL homodimerization. This could constitute a mechanistic basis for the ability of AR-Vs to attenuate androgen induction of AR-FL activity (5). To date, functional studies of AR-Vs have been focused mostly on their ability to regulate gene expression independent of AR-FL. Because AR-Vs are often coexpressed with AR-FL in biologic contexts, it is conceivable that the ability of AR-Vs to heterodimerize with and activate AR-FL in an androgen-independent manner could be equally important as their AR-FL–independent activity to castration resistance.

We and others showed previously that AR-V7 and AR^{v567es} localize constitutively to the nucleus and can facilitate AR-FL nuclear entry (5, 15), indicating that the initial interaction between AR-V and AR-FL is likely to be in the cytoplasm. This is supported by our data showing both cytoplasmic and nuclear localization of AR^{v567es}/AR-FL dimerization. Intriguingly, AR-V7/AR-FL dimerization is detected primarily in the nucleus in the vast majority of the cells. This may be due to the regeneration of the Venus fluorescent protein from the VN and VC fragments being slower than AR-V7/AR-FL nuclear translocation. Interestingly, AR-V7/AR-V7 dimerization was also detected primarily in the nucleus, whereas AR^{v567es}/AR^{v567es} and AR-V7/AR^{v567es} dimerization were observed in both the nucleus and the cytoplasm. Whether this is also due to slower regeneration of the Venus fluorescent protein than AR-V7/AR-V7 nuclear translocation or AR-V7 entering the nucleus as a monomer requires further investigation. In addition, the majority of the posttranslational modification sites of AR-FL are retained in AR-Vs (34). These posttranslational modifications regulate AR-FL transactivating activity, possibly via the interaction of AR-FL with other proteins or with itself (34). It is very likely that these posttranslational modifications may impact AR-V dimerization and transactivation and therefore deserve further investigation.

We reported previously that AR-V binds to the promoter of its specific target UBE2C without AR-FL, but co-occupies the promoter of the canonical AR target PSA with AR-FL in a mutually dependent manner (5). Furthermore, knockdown of AR-FL and AR-V both result in reduced androgen-independent PSA expression, but only AR-V knockdown downregulates UBE2C expression (5). The data, together with the findings from the current study, indicate that AR-Vs regulate their specific targets as an AR-V/AR-V dimer but control the expression of canonical AR targets as an AR-V/AR-FL dimer. Interestingly, while mutating D-box alone does not significantly mitigate AR-V/AR-FL dimerization, the mutation abolishes the ability of AR-V to induce the expression of PSA and UBE2C as well as to promote castration-resistant cell growth. A plausible explanation is that, although D-box–mutated AR-V can dimerize with AR-FL, the dimer cannot bind to DNA to regulate the expression of target genes. This, together with the finding that D-box–D-box interactions are required for the formation of androgen-induced AR-FL intermolecular N/C

Published OnlineFirst June 9, 2015; DOI: 10.1158/0008-5472.CAN-15-0381

interactions (32), indicates that disrupting D-box–D-box interactions could lead to inhibition of not only AR-V/AR-V dimerization and transactivation but also AR-FL activation induced by either AR-Vs or androgens. Thus, disrupting D-box–D-box interactions may represent a more effective means to suppress AR signaling than targeting the LBD of AR.

In summary, we demonstrated the dimeric nature of AR-Vs in live cells and identified the dimerization interface. Significantly, we showed that proper dimerization is required for AR-V functions. The research therefore represents a key step in delineating the mechanism by which AR-Vs mediate gene regulation. This is vital for developing effective therapeutic strategies to disrupt AR-V signaling and provide more effective treatments for prostate cancer.

Disclosure of Potential Conflicts of Interest

O. Sartor is a consultant/advisory board member for Astellas, Janssen, and Medivation. No potential conflicts of interest were disclosed by the other authors.

Authors' Contributions

Conception and design: D. Xu, Y. Zhan, Y. Qi, B. Cao, H. Zhang, Y. Dong
Development of methodology: D. Xu, Y. Zhan, Y. Qi, S.S. Gambhir, H. Zhang
Acquisition of data (provided animals, acquired and managed patients, provided facilities, etc.): D. Xu, S. Bai
Analysis and interpretation of data (e.g., statistical analysis, biostatistics, computational analysis): D. Xu, Y. Qi, S. Bai, P. Lee, Y. Dong
Writing, review, and/or revision of the manuscript: D. Xu, Y. Zhan, B. Cao, W. Xu, S.S. Gambhir, P. Lee, O. Sartor, E.K. Flemington, H. Zhang, Y. Dong
Administrative, technical, or material support (i.e., reporting or organizing data, constructing databases): D. Xu
Study supervision: Y. Qi, W. Xu, Y. Dong
Other (provided BiFC plasmids and suggestions to conduct the BiFC experiments. Also, reviewed the manuscript with comments): C.-D. Hu

Acknowledgments

The authors thank Dr. Yun Qiu (University of Maryland, College Park, MD) for the human AR-FL and AR-V7 expression constructs, Dr. Stephen Plymate (University of Washington, Seattle, WA) for the human AR^{v567es} expression construct, Dr. Jun Luo (Johns Hopkins University, Baltimore, MD) for the pEGFP-AR construct, Drs. Zhou Songyang and Nancy L. Weigel (Baylor College of Medicine, Houston, TX) for the pHAGE-Ind-EF1a-DEST-GH construct, and Dr. Shahriar Koochekpour (Roswell Park Cancer Institute, Buffalo, NY) for C4-2 cells. The authors appreciate the excellent technical assistance from Ms. Mary Price at the Louisiana Cancer Research Consortium FACS Core.

Grant Support

This work was supported by the following grants: NIH/NCI R01CA188609, NIH/NIGMS P20GM103518, DOD W81XWH-12-1-0112, W81XWH-14-1-0485, and W81XWH-12-1-0275; Louisiana Board-of-Regents LEQSF (2012–15)-RD-A-25; the Louisiana Cancer Research Consortium Fund; the Tulane University School of Medicine Research Bridge Fund; and the National Natural Science Foundation of China Projects 81272851 and 81430087.

The costs of publication of this article were defrayed in part by the payment of page charges. This article must therefore be hereby marked *advertisement* in accordance with 18 U.S.C. Section 1734 solely to indicate this fact.

Received February 6, 2015; revised May 7, 2015; accepted May 27, 2015; published OnlineFirst June 9, 2015.

References

1. Egan A, Dong Y, Zhang H, Qi Y, Balk SP, Sartor O. Castration-resistant prostate cancer: adaptive responses in the androgen axis. Cancer Treat Rev 2014;40:426–33.
2. Knudsen KE, Scher HI. Starving the addiction: new opportunities for durable suppression of AR signaling in prostate cancer. Clin Cancer Res 2009;15:4792–8.
3. Fizazi K, Scher HI, Molina A, Logothetis CJ, Chi KN, Jones RJ, et al. Abiraterone acetate for treatment of metastatic castration-resistant prostate cancer: final overall survival analysis of the COU-AA-301 randomised, double-blind, placebo-controlled phase 3 study. Lancet Oncol 2012;13:983–92.
4. Scher HI, Fizazi K, Saad F, Taplin ME, Sternberg CN, Miller K, et al. Increased survival with enzalutamide in prostate cancer after chemotherapy. N Engl J Med 2012;367:1187–97.
5. Cao B, Qi Y, Zhang G, Xu D, Zhan Y, Alvarez X, et al. Androgen receptor splice variants activating the full-length receptor in mediating resistance to androgen-directed therapy. Oncotarget 2014;5:1646–56.
6. Dehm SM, Schmidt LJ, Heemers HV, Vessella RL, Tindall DJ. Splicing of a novel androgen receptor exon generates a constitutively active androgen receptor that mediates prostate cancer therapy resistance. Cancer Res 2008;68:5469–77.
7. Guo Z, Yang X, Sun F, Jiang R, Linn DE, Chen H, et al. A novel androgen receptor splice variant is up-regulated during prostate cancer progression and promotes androgen depletion-resistant growth. Cancer Res 2009;69:2305–13.
8. Hornberg E, Ylitalo EB, Crnalic S, Antti H, Stattin P, Widmark A, et al. Expression of androgen receptor splice variants in prostate cancer bone metastases is associated with castration-resistance and short survival. PLoS ONE 2011;6:e19059.
9. Hu R, Dunn TA, Wei S, Isharwal S, Veltri RW, Humphreys E, et al. Ligand-independent androgen receptor variants derived from splicing of cryptic exons signify hormone-refractory prostate cancer. Cancer Res 2009;69:16–22.
10. Hu R, Lu C, Mostaghel EA, Yegnasubramanian S, Gurel M, Tannahill C, et al. Distinct transcriptional programs mediated by the ligand-dependent full-length androgen receptor and its splice variants in castration-resistant prostate cancer. Cancer Res 2012;72:3457–62.
11. Li Y, Chan SC, Brand LJ, Hwang TH, Silverstein KA, Dehm SM. Androgen receptor splice variants mediate enzalutamide resistance in castration-resistant prostate cancer cell lines. Cancer Res 2012;73:483–9.
12. Liu LL, Xie N, Sun S, Plymate S, Mostaghel E, Dong X. Mechanisms of the androgen receptor splicing in prostate cancer cells. Oncogene 2014;33:3140–50.
13. Mostaghel EA, Marck BT, Plymate SR, Vessella RL, Balk S, Matsumoto AM, et al. Resistance to CYP17A1 inhibition with abiraterone in castration-resistant prostate cancer: induction of steroidogenesis and androgen receptor splice variants. Clin Cancer Res 2011;17:5913–25.
14. Nadiminty N, Tummala R, Liu C, Yang J, Lou W, Evans CP, et al. NF-kappaB2/p52 induces resistance to enzalutamide in prostate cancer: role of androgen receptor and its variants. Mol Cancer Ther 2013;12:1629–37.
15. Sun S, Sprenger CC, Vessella RL, Haugk K, Soriano K, Mostaghel EA, et al. Castration resistance in human prostate cancer is conferred by a frequently occurring androgen receptor splice variant. J Clin Invest 2010;120:2715–30.
16. Zhang X, Morrissey C, Sun S, Ketchandji M, Nelson PS, True LD, et al. Androgen receptor variants occur frequently in castration resistant prostate cancer metastases. PLoS ONE 2011;6:e27970.
17. Antonarakis ES, Lu C, Wang H, Luber B, Nakazawa M, Roeser JC, et al. AR-V7 and resistance to enzalutamide and abiraterone in prostate cancer. N Engl J Med 2014;371:1028–38.
18. Zhang H, Zhan Y, Liu X, Qi Y, Zhang G, Sartor O, et al. Splicing variants of androgen receptor in prostate cancer. Am J Clin Exp Urol 2013;1:18–24.
19. Hu R, Isaacs WB, Luo J. A snapshot of the expression signature of androgen receptor splicing variants and their distinctive transcriptional activities. Prostate 2011;71:1656–67.
20. Watson PA, Chen YF, Balbas MD, Wongvipat J, Socci ND, Viale A, et al. Constitutively active androgen receptor splice variants expressed in castration-resistant prostate cancer require full-length androgen receptor. Proc Natl Acad Sci U S A 2010;107:16759–65.

21. Chan SC, Li Y, Dehm SM. Androgen receptor splice variants activate androgen receptor target genes and support aberrant prostate cancer cell growth independent of canonical androgen receptor nuclear localization signal. J Biol Chem 2012;287:19736–49.
22. Centenera MM, Harris JM, Tilley WD, Butler LM. Minireview: the contribution of different androgen receptor domains to receptor dimerization and signaling. Mol Endocrinol 2008;22:2373–82.
23. Hu CD, Grinberg AV, Kerppola TK. Visualization of protein interactions in living cells using bimolecular fluorescence complementation (BiFC) analysis. Curr Protoc Cell Biol 2006; Chapter 21:Unit 21.3.
24. Dragulescu-Andrasi A, Chan CT, De A, Massoud TF, Gambhir SS. Bioluminescence resonance energy transfer (BRET) imaging of protein–protein interactions within deep tissues of living subjects. Proc Natl Acad Sci U S A 2011;108:12060–5.
25. Pfleger KDG, Seeber RM, Eidne KA. Bioluminescence resonance energy transfer (BRET) for the real-time detection of protein–protein interactions. Nat Protocols 2006;1:337–45.
26. Liu S, Qi Y, Ge Y, Duplessis T, Rowan BG, Ip C, et al. Telomerase as an important target of androgen signaling blockade for prostate cancer treatment. Mol Cancer Ther 2010;9:2016–25.
27. Dong Y, Zhang H, Gao AC, Marshall JR, Ip C. Androgen receptor signaling intensity is a key factor in determining the sensitivity of prostate cancer cells to selenium inhibition of growth and cancer-specific biomarkers. Mol Cancer Ther 2005;4:1047–55.
28. Zhan Y, Cao B, Qi Y, Liu S, Zhang Q, Zhou W, et al. Methylselenol prodrug enhances MDV3100 efficacy for treatment of castration-resistant prostate cancer. Int J Cancer 2013;133:2225–33.
29. Dong Y, Zhang H, Hawthorn L, Ganther HE, Ip C. Delineation of the molecular basis for selenium-induced growth arrest in human prostate cancer cells by oligonucleotide array. Cancer Res 2003;63:52–9.
30. Dong Y, Lee SO, Zhang H, Marshall J, Gao AC, Ip C. Prostate specific antigen expression is downregulated by selenium through disruption of androgen receptor signaling. Cancer Res 2004;64:19–22.
31. Vichai V, Kirtikara K. Sulforhodamine B colorimetric assay for cytotoxicity screening. Nat Protoc 2006;1:1112–6.
32. van Royen ME, van Cappellen WA, de VC, Houtsmuller AB, Trapman J. Stepwise androgen receptor dimerization. J Cell Sci 2012;125:1970–9.
33. Hamdan FF, Percherancier Y, Breton B, Bouvier M. Monitoring protein–protein interactions in living cells by bioluminescence resonance energy transfer (BRET). Curr Protoc Neurosci 2006;Chapter 5:UNit 5.23.
34. van der Steen T, Tindall DJ, Huang H. Posttranslational modification of the androgen receptor in prostate cancer. Int J Mol Sci 2013;14:14833–59.